Title
Measurements of reactive nitrogen produced by tropical thunderstorms during BIBLE-C

Journal
Journal of Geophysical Research, 112(D18)

ISSN
0148-0227

Authors
Koike, M
Kondo, Y
Kita, K
et al.

Publication Date
2007

DOI
10.1029/2006jd008193

Measurements of reactive nitrogen produced by tropical thunderstorms during BIBLE-C

M. Koike,[1] Y. Kondo,[2] K. Kita,[3] N. Takegawa,[2] N. Nishi,[4] T. Kashihara,[1] S. Kawakami,[5] S. Kudoh,[1] D. Blake,[6] T. Shirai,[7] B. Liley,[8] M. Ko,[9] Y. Miyazaki,[2] Z. Kawasaki,[10] and T. Ogawa[5]

Received 28 October 2006; revised 22 April 2007; accepted 22 June 2007; published 19 September 2007.

[1] The Biomass Burning and Lightning Experiment phase C (BIBLE-C) aircraft mission was carried out near Darwin, Australia (12°S, 131°E) in December 2000. This was the first aircraft experiment designed to estimate lightning NO production rates in the tropics, where production is considered to be most intense. During the two flights (flights 10 and 13 made on December 9 and 11–12, respectively) enhancements of NO_x ($NO + NO_2$) up to 1000 and 1600 parts per trillion by volume (pptv, 10-s data) were observed at altitudes between 11.5 and 14 km. The Geostationary Meteorological Satellite (GMS) cloud (brightness temperature) data and ground-based lightning measurements by the Global Positioning and Tracking System (GPATS) indicate that there were intensive lightning events over the coast of the Gulf of Carpentaria, which took place upstream from our measurement area 10 to 14 h prior to the measurements. For these two flights, air in which NO_x exceeded 100 pptv extended over 620×140 and 400×170 km^2 (wind direction $\times$ perpendicular direction), respectively, suggesting a significant impact of lightning NO production on NO_x levels in the tropics. We estimate the amount of NO_x observed between 11.5 and 14 km produced by the thunderstorms to be 3.3 and 1.8×10^{29} NO molecules for flights 10 and 13, respectively. By using the GPATS lightning flash count data, column NO production rates are estimated to be 1.9–4.4 and $21–49 \times 10^{25}$ NO molecules per single flash for these two flight data sets. In these estimations, it is assumed that the column NO production between 0 and 16 km is greater than the observed values between 11.5 and 14 km by a factor of 3.2, which is derived using results reported by Pickering et al. (1998). There are however large uncertainties in the GPATS lightning data in this study and care must be made when the production rates are referred. Uncertainties in these estimates are discussed. The impact on the ozone production rate is also described.

Citation: Koike, M., et al. (2007), Measurements of reactive nitrogen produced by tropical thunderstorms during BIBLE-C, *J. Geophys. Res.*, *112*, D18304, doi:10.1029/2006JD008193.

1. Introduction

[2] It is widely recognized that NO production by lightning has a significant impact on the global NO_x (= NO + NO_2) distribution. Although its source strength is considered to be smaller compared to emissions from fossil fuel combustion (5 versus 33 Tg(N) yr^{-1} [*IPCC*, 2001]), it still has a significant impact because lightning NO is produced in the free troposphere, where the lifetime of NO_x is longer than in the boundary layer where most anthropogenic NO_x is emitted. Its relative contribution among NO_x sources is particularly large in the tropics [*Lamarque et al.*, 1996; *Wang et al.*, 1998; *Levy et al.*, 1999; *Nesbitt et al.*, 2000; *Tie et al.*, 2001; *Bond et al.*, 2002; *Labrador et al.*, 2005] because 80% of lightning occurs between 30°S and 30°N latitude [*Christian et al.*, 2003] and anthropogenic NO_x sources are smaller there compared to the northern midlatitudes. Therefore in order to better understand tropospheric chemistry it is essential to quantify the source strength,

[1]Department of Earth and Planetary Science, Graduate School of Science, The University of Tokyo, Tokyo, Japan.
[2]Research Center for Advanced Science and Technology, The University of Tokyo, Tokyo, Japan.
[3]Department of Environmental Science, Graduate School of Science, Ibaraki University, Ibaraki, Japan.
[4]Department of Earth and Planetary Science, Graduate School of Science, Kyoto University, Kyoto, Japan.
[5]Earth Observation Research and Application Center, Japan Aerospace Exploration Agency, Tokyo, Japan.
[6]University of California-Irvine, Irvine, California, USA.
[7]National Institute for Environmental Studies, Ibaraki, Japan.
[8]National Institute of Water and Atmospheric Research Ltd, Lauder, New Zealand.
[9]NASA Langley Research Center, Hampton, Virginia, USA.
[10]Department of Communications Engineering, Graduate School of Engineering, Osaka University, Osaka, Japan.

0148-0227/07/2006JD008193

spatial distribution, and vertical distribution of lightning-produced NO_x from thunderstorm events [*Labrador et al.*, 2005]. Despite its importance, however, the range of uncertainties of these quantities is quite large as compared to other NO_x sources.

[3] In global chemistry transport model (CTM) calculations, the lightning NO production rate is generally expressed by three parameters: global source strength (the total amount of NO produced by lightning per year), horizontal distribution, and vertical distribution. The global source strength is generally used as a constraint in the models, because when the horizontal distribution of lightning NO production is calculated using a certain parameterization, the total amount of NO produced needs to be scaled to match this constraint. Numerous studies have been done to estimate the global source strength, and this will be described further below. For horizontal distribution, an empirical parameterization developed by *Price and Rind* [1992] in which the lightning flash rate is expressed as a function of convective cloud top height for both continental and marine clouds, is widely used (e.g., summarized in Table 1 in *Zhang et al.* [2003]). The convective mass flux has also been used to parameterize the lightning flash rate in order to account for differences in flash rates and vertical velocities between continental and marine storms [*Grewe et al.*, 2001; *Allen and Pickering*, 2002]. Because of the altitude dependence of the NO_x lifetime and its impact on chemistry, the vertical profile of produced NO is also a very important parameter for global models [*Pickering et al.*, 1998; *Labrador et al.*, 2005]. However, the uncertainty in the location of NO production in a storm system and the vertical redistribution process of produced NO by vertical transport of air within a storm system prevent making a simple assumption. Using a two-dimensional model, *Pickering et al.* [1998] derived a vertical NO_x distribution for the conditions at the end of the storm for various storm types. These vertical distributions have been used in several global models, although very simple assumptions, such as a constant mixing ratio distribution, have also been widely used.

[4] An important factor in controlling both horizontal and vertical NO distributions is the ratio between flash counts of intra-cloud (IC, which includes cloud-to-cloud) and cloud-to-ground (CG) flashes (N_{IC}/N_{CG}) and the ratio of their NO production rates by a single flash (P_{IC}/P_{CG}), because the total NO production ($N_{IC}\,P_{IC} + N_{CG}\,P_{CG}$) depends on these quantities. An empirical parameterization developed by *Price and Rind* [1993] is widely used for the N_{IC}/N_{CG} ratio (equation (4) in section 4.7). For the ratio of NO production rates between IC and CG flashes, P_{IC}/P_{CG}, a value of 0.1 proposed by *Price et al.* [1997] has been used in various global CTM calculations (summarized in Table 1 in *Zhang et al.* [2003]). Recent observations, on the other hand, suggest that P_{IC}/P_{CG} is likely greater, possibly as large as unity [*DeCaria et al.*, 2000; *Fehr et al.*, 2004]. Considering the estimate that the peak current of IC flashes is an order of magnitude less than that for CG flashes, this suggests that the total channel length of an IC flash would be more than 10 times that of a CG flash [*DeCaria et al.*, 2000]. Because the N_{IC}/N_{CG} ratio changes depending on location and season (e.g., the parameterization by *Price and Rind* [1993]), the use of a different P_{IC}/P_{CG} value results in different spatial and temporal variations of a lighting NO source strength.

[5] Although a global source strength of lightning NO production is used as a constraint in most global model calculations, the range of previous estimates is quite large: 0.7–220 Tg(N) yr^{-1} [*Huntrieser et al.*, 1998]. The global source strength of lightning NO production (G in units of Tg(N) yr^{-1}) is estimated based on the following expression:

$$G = fP \tag{1}$$

where P is the NO mass produced by a single event (e.g., lightning flash, thunderstorm, unit mass flux out from the cloud anvil) and f is the global occurrence frequency of the events. NO production per lightning flash is widely used for this expression, because the global lightning flash frequency has been reasonably well estimated from direct measurements of the flash rate from satellites, such as the Optical Transient Detector (OTD). Both CG and IC flashes are considered to be detected by this instrument, and on average 44 ± 5 flashes ($f_{CG} + f_{IC}$) occur around the globe every second [*Christian et al.*, 2003]. If one can estimate the NO production rate based on a single lightning flash (P), a global production rate (G) can be calculated. When one considers the different NO production rates for CG and IC flashes (P_{CG} and P_{IC}), then equation (1) can be written using the CG and IC flash rates (f_{CG} and f_{IC}) as follows.

$$G = f_{CG}\,P_{CG} + f_{IC}\,P_{IC} \tag{2}$$

[6] The lightning NO production rate by a single flash event P has been estimated from laboratory studies [e.g., *Wang et al.*, 1998], satellite measurements [*Boersma et al.*, 2005], and field studies [e.g., *Ridley et al.*, 1996; *Huntrieser et al.*, 1998; *Höller et al.*, 1999; *DeCaria et al.*, 2000; *Huntrieser et al.*, 2002; *Skamarock et al.*, 2003; *Fehr et al.*, 2004; *Ridley et al.*, 2004]. Because of both the great importance and uncertainties in production estimates, several aircraft experiments focusing on the evaluation of the production rate have been conducted. From measurements of isolated thunderstorms over New Mexico, *Ridley et al.* [1996] estimated the number of NO molecules produced by a single lightning flash (average of CG and IC flashes) to be 2.9–3.5 × 10^{25} NO molecules $flash^{-1}$ in the upper troposphere (Table 1). More comprehensive measurements were made during the Stratospheric-Tropospheric Experiment: Radiation, Aerosols, and Ozone (STERAO)-Deep Convection experiment over Colorado [*Dye et al.*, 2000]. From this experiment, a factor of 10 difference in estimates was derived depending on the event and methods of estimation (Table 1): 2.6 × 10^{25} NO molecules $flash^{-1}$ (CG + IC) was derived by *Skamarock et al.* [2003], while *DeCaria et al.* [2000] showed that the CG flash yields 12–60 × 10^{25} NO molecules $flash^{-1}$ and a production rate of IC flash was similar to that of CG flash. During the Cirrus Regional Study of Tropical Anvils and Cirrus Layers – Florida Area Cirrus Experiment (CRYSTAL-FACE) a factor of 4–5 different production rate was also obtained; 3.3–6.6 and 17–23 × 10^{25} NO molecules $flash^{-1}$ were derived for moderately and highly active storms (Table 1) [*Ridley et al.*, 2004]. In these estimations different methods were used

Table 1. Comparison of Lightning Activity and Produced NO_x Amounts

Experiment	BIBLE-C	BIBLE-C	New Mexico	STERAO-A	STERAO-A	CRYSTAL-FACE	CRYSTAL-FACE	LINOX	EULINOX
Location	Darwin	Darwin	New Mexico	Colorado	Colorado	Florida	Florida	Germany	Germany
References	This study	This study	*Ridley et al.* [1996]	*Dye et al.* [2000]; *Defer et al.* [2001]; *Skamarock et al.* [2003]	*DeCaria et al.* [2000]	*Ridley et al.* [2004]	*Ridley et al.* [2004]	*Huntrieser et al.* [1998]; *Höller et al.* [1999]	*Fehr et al.* [2004]; *Huntrieser et al.* [1998]
Event	Flight 10	Flight 13	August 12 & 19	July 10	July 12	July 16	July 29	average	average
Storm size, km^2[a]	190 × 120	190 × 70	75 × 30[b]	100 × 50[b]	100 × 45[b]	4200	15000	3000[b,c]	2000[b,d]
Storm duration, h	3	2	2[b]	3[b]	3[b]	2[b]	3[b]	2[b,c]	3[b,d]
CG flashes	3260 (1410)[e]	402 (171)[e]	135–168	83	155	392	3067	2000[b,c]	244[d]
CG + IC flashes	57,400 (24,900)[e]	2750 (1170)[e]	337–420[f]	5428[g]	1263[g]	1274[f]	9967[f]	———	3321[d,g]
Produced NO_x (10^{28} molecules)	32.8 (11.5–14 km)	17.9 (11.5–14 km)	1.2 (8–11.8 km)	14–38	———	4.2–8.4 (6–14.5 km)	170–230 (5–14 km)	0.86–6.0	1.5–2.2[h] 27 (0.70–100)[i]
NO production rate (10^{25} molecules/flash)	1.88–4.35	21.0–49.3	2.9–3.5 (8–11.8 km)	2.6	12–30[j]	3.3–6.6 (6–14.5 km)	17–23 (5–14 km)	4–30[k]	8.1 (0.21–30)
Global NO production rate (Tg(N)/yr)[l]	0.62–1.43	6.9–16.3	0.92–1.1	0.8	4.0–9.9	1.1–2.2	5.5–7.5	2–4	2.7 (0.07–9.9)

[a]Storm size is estimated based on anvil size.
[b]These values are estimated from the descriptions and/or cloud image pictures in the original papers by the authors of this study.
[c]July 23 event.
[d]July 21 event.
[e]Values without parentheses are derived by assuming that all the GPATS-detected lightning flashes are CG flashes. Values within the parentheses are derived by assuming that 60% of positive flashes detected by GPATS are IC flashes. See text for details (sections 2.2 and 4.7). Total lightning flash number ($N_{IC} + N_{CG}$) was estimated from CG flash number and empirical parameterization developed by *Price and Rind* [1993] (equation (4)).
[f]Total lightning flash number ($N_{IC} + N_{CG}$) was estimated from the CG flash number and climatological N_{IC}/N_{CG} ratio.
[g]IC flash detected by the VHF interferometer operated by the French ONERA.
[h]This is estimated by the authors of this study by using an average NO_x concentration in the anvil of 0.9 ppbv and an average air flux from the anvil of 1.1×10^8 kg s^{-1} [*Huntrieser et al.*, 2002] and by assuming a thunderstorm duration of 2 to 3 h.
[i]This is estimated by the authors of this study by using an average NO production rate per single lightning flash [*Huntrieser et al.*, 2002] and total flash counts observed for the July 21 thunderstorm by the VHF interferometer operated by the French ONERA [*Fehr et al.*, 2004].
[j]Production rate for CG flash. $P_{IC}/P_{CG} = 0.5–1.0$ was also suggested.
[k]Climatological flash count is used for this estimate.
[l]These estimates are made by the authors of this study using the global lightning flash frequency of 44 flashes s^{-1} [*Christian et al.*, 2003], although a different frequency is used in some original studies.

to estimate IC flash count from CG flash count, and therefore, a comparison of NO production rates must be made carefully (this issue will be discussed in section 4.9).

[7] Despite the great contribution of lightning NO production in the tropics, systematic measurements of lightning NO production have been carried out only at midlatitudes and never in the tropics. The BIomass Burning and Lightning Experiment phase C (BIBLE-C) was conducted over northern Australia between November 24 and December 15, 2000, using a Gulfstream II (G-II) aircraft. This experiment was conducted as the third of the series of BIBLE projects, which were described by *Kondo et al.* [2002]. In total eight intensive flights were made over northern Australia using Darwin (12°S, 131°E) as a base airport. Lightning activity was monitored using the ground-based Lightning Position and Tracking System (LPATS) implemented by the Global Positioning and Tracking Systems Pty Ltd (GPATS) in Australia. During the BIBLE-C experiment, we successfully obtained data that show clear signatures of lightning NO production during two flights, flight 10 (December 9, 2000) and 13 (December 11–12, 2000). In this paper, results from these two flights are described in detail and an estimate of lightning NO production rate by a single lightning flash is shown.

2. Measurements

2.1. Aircraft Measurements

[8] During BIBLE-C, NO and total reactive nitrogen (NO_y), which is considered to include NO + NO_2 + NO_3 + HNO_2 + HNO_3 + HNO_4 + $2N_2O_5$ + PAN + other organic nitrates + aerosol nitrates, were measured together with O_3, CO, CO_2, H_2O, CH_4, various non methane hydrocarbons (NMHCs), selected halocarbons, condensation nuclei (CN), aerosol size distribution, and actinic flux for NO_2 photolysis ($J(NO_2)$). Both NO and NO_y were measured using an NO-O_3 chemiluminescence technique [*Kondo et al.*, 1997]. NO_y compounds were catalytically converted to NO on the surface of a heated gold tube (300°C) with the addition of CO. The NO and NO_y instrument used for BIBLE-C was very similar to that used during BIBLE-A, conducted in 1998 [*Koike et al.*, 2002a], and it was used with some modifications during NASA's Subsonic ASSessment (SASS) Ozone and NO_x EXperiment (SONEX) [*Koike et al.*, 2000], the SAGE III Ozone Loss and Validation Experiment (SOLVE) [*Koike et al.*, 2002b], and the Transport and Chemical Evolution over the Pacific (TRACE-P) experiments [*Koike et al.*, 2003; *Miyazaki et al.*, 2005]. During the BIBLE-A and -C experiments, the NO_y converter unit was placed underneath the aircraft cabin so as to minimize the length of the inlet Teflon tube for air sampling upstream of the gold tube converter. The inlet tube, which was heated to 60°C, faced rearward, discriminating against particles of diameter larger than about 1 μm. Data were recorded every 1-s, however 10-s averaged data were used in this study. The precisions of the 10-s NO and NO_y measurements at 10 km estimated from the photon count fluctuations (1σ) were 2 and 3 parts per trillion by volume (pptv) for NO and NO_y values of 100 and 200 pptv, respectively. The absolute accuracies were estimated to be 8 and 17% for these NO and NO_y values.

[9] Carbon monoxide (CO) concentrations were measured using a vacuum ultraviolet (VUV) resonance fluorescence technique [*Takegawa et al.*, 2001]. The precision of the 10-s data (1σ) and absolute accuracy were 3 parts per billion by volume (ppbv) and 5%, respectively. Measurements of O_3 were made using a dual-beam UV absorption photometer developed at the University of Tokyo [*Kita et al.*, 2002]. The precision of the 10-s data (1σ) and absolute accuracy were 0.9 ppbv and 5%, respectively. The concentrations of CH_4, various NMHCs, selected halocarbons, and C_1-C_4 alkyl nitrates were measured by collecting whole air samples and analyzing them using gas chromatography with flame ionization, electron capture, and mass spectrometer detection. Sample filling time ranged from 0.5 to 3 min and samples were collected every 2–5 min on average. The detection limit of the whole air measurements is summarized by *Simpson et al.* [2000]. The $J(NO_2)$ values were measured using two sets of filter radiometers; one set looked upward and the other looked downward from the aircraft (Meteorologie Consult, Glashutte, Germany) [*Volz-Thomas et al.*, 1996; *Kita et al.*, 2002].

[10] The photostationary-state NO_2 mixing ratios were calculated using a box model developed at Atmospheric and Environmental Research Inc. [*Ko et al.*, 2002] from the observed values of atmospheric temperature, pressure, NO, O_3, CO, CH_4, H_2O, NMHCs, and $J(NO_2)$ for periods when the solar zenith angles were smaller than 80°. The median NO/NO_x ratio at an altitude of 12.5 km during flight 10 was 0.95, indicating that an error in the NO_2 estimation has little effect on NO_x estimation.

[11] In this paper, 10-s data are used if not otherwise stated. To calculate NO_2 mixing ratios for every 10-s, NMHC data were interpolated.

2.2. Ground-Based Lightning Measurements

[12] During the BIBLE-C experiment, lightning activity was monitored by the LPATS system operated by GPATS in Australia. The LPATS system uses difference-of-arrival-time techniques to identify the location of a lightning stroke by receiving LF electromagnetic radiation from the return stroke at three or more receiving stations. The LPATS system is supposed to detect only CG strokes. The GPATS network in Australia consisted of 22 receivers when the BIBLE-C experiment was conducted (Figure 1). Most of them were located on the east coast of Australia and the closest station to the area in which we made aircraft measurements was located at Tennant Creek (19.6°S and 134.2°E). For the two thunderstorms that we focus on in this study (thunderstorms for flights 10 and 13, as described later), the distances between the center of the thunderstorm and this station were 430 and 610 km, respectively. In this study lightning flash data sets were constructed from lightning stroke data.

[13] The LPATS system has also been used in the US and in European countries. The efficiency of the US National Lightning Detection Network (NLDN), which also uses modified LPATS sensors, was reported to be 80–90% for CG events with peak currents above 5 kA [*Cummins et al.*, 1998]. During the EULINOX experiment, signals detected by the LPATS system in Germany were compared with a VHF interferometer [*Thery*, 2001]. As a result, it was found that nearly all "real negative CG strokes" were recorded by

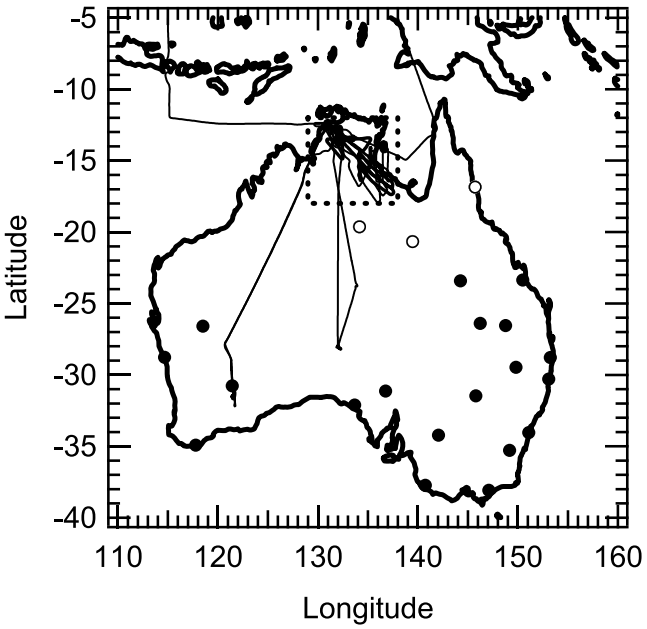

Figure 1. Flight tracks for the research aircraft during the BIBLE-C experiment. The study area is shown with a rectangle (dashed line). Locations of GPATS receivers are shown by open and closed circles. Open circles show locations of GPATS receivers which were used to detect lighting flashes around the study area; Cairns (16.9°S, 145.7°E), Tennant Creek (19.6°S, 134.2°E), and Mt. Isa (20.7°S, 139.5°E).

the LPATS system (detection efficiency of 100%), however 32% of LPATS negative flashes were in fact IC flashes. Similarly, 61% of LPATS positive flashes (those of low intensity) were found to be IC flashes.

[14] It is commonly reported that most CG flashes are negative [e.g., *Uman*, 1987; *MacGorman and Rust*, 1998]. Based on 5000 CG flashes associated with eight mesoscale convective systems observed at Darwin during the Down Under Doppler and Electricity Experiment (DUNDEE), *Petersen and Rutledge* [1992] reported that 91% of CG flashes were negative. Statistical analyses of CG flashes detected over the US by NLDN between 1995 and 1999 also showed that 90% of the CG flashes were negative [*Zajac and Rutledge*, 2001]. However, for the two thunderstorms that we focus on in this study (thunderstorms for flights 10 and 13, as described later), GPATS measurements indicate that negative flashes constituted only 5.7 and 4.3%, respectively, and the rest of flashes were positive. Furthermore, statistical analyses on one month GPATS data (December 2000) around the area which we studied (12–18°S and 132–140°E), indicate that, of 82400 flashes, only 20% were negative (Table A1 in Appendix). Considering these results, there is a possibility that some negative CG flashes detected near Darwin by the Australian GPATS during BIBLE-C were mislabeled as positive CG flashes and/or a portion of the IC flashes were mislabeled as positive CG flashes. In the latter case, we would overestimate the number of CG flashes and therefore the total number of flashes calculated from the CG flash number, which is used to estimate the lightning NO production rate per single flash. In Appendix A, results from additional analyses showing possible errors in GPATS CG/IC labeling are presented. It is difficult, however, to estimate the fraction of CG/IC mislabeling, especially when GPATS receivers are located relatively far from Darwin (Figure 1). *Thery* [2001] showed that IC flashes, which had been mislabeled as positive CG flashes by LPATS, generally had low current intensities, and these flashes are considered to be difficult to detect with GPATS receivers located far from Darwin in our case. Possible errors in the estimation of lightning NO production due to this overestimation of the lightning flash counts will be discussed in section 4.7. Because of these uncertainties in the detection of lightning flashes by GPATS, we have made no correction for detection efficiency. In this paper, we will describe flashes detected by the GPATS

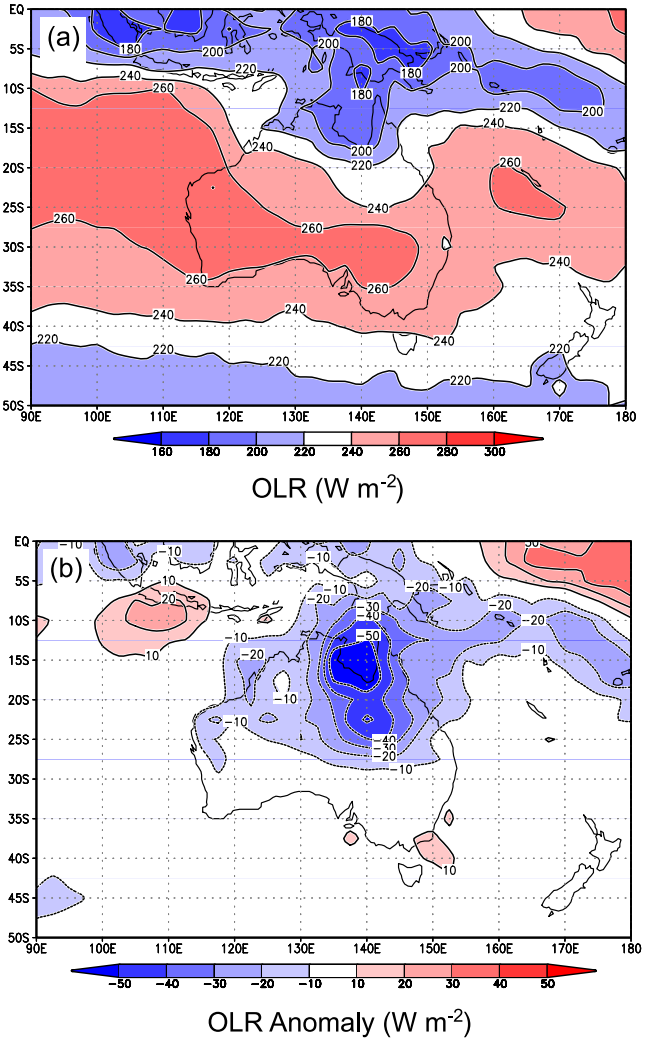

Figure 2. (a) Monthly average outgoing long-wave radiation (OLR, W m^{-2}) for December 2000. (b) Anomaly in December 2000 from the 30-year average (1970–2000). Interpolated OLR data were provided by NOAA/OAR/ESRL PSD, Boulder, Colorado, USA, from their Web site at http://www.cdc.noaa.gov/.

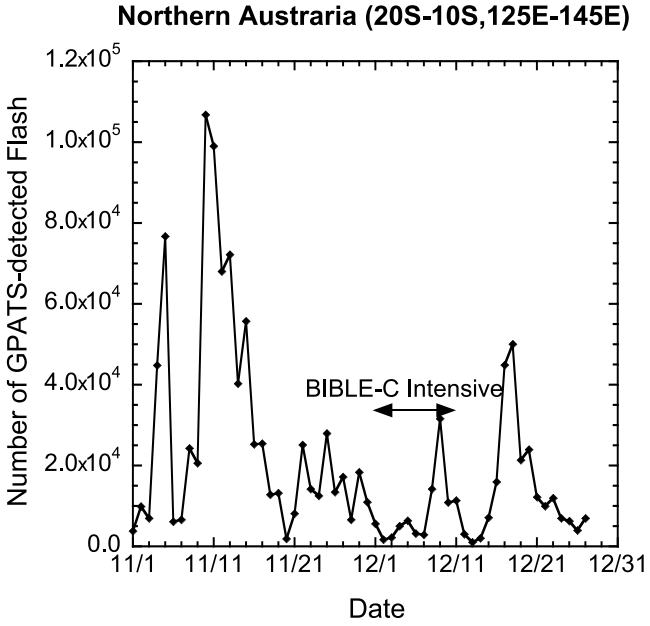

Figure 3. Daily number of lightning flashes over northern Australia (10–20°S, 125–145°E) as detected by the GPATS system. The period of the BIBLE-C observations made in the study area is shown with an arrow.

system as "GPATS-detected flashes", rather than "CG flashes".

3. Meteorological Conditions

[15] In the austral summer of 2000–2001, the transition from the pre-monsoon to monsoon season (or wet season) started earlier than average and the BIBLE-C measurements were made in the monsoon regime. During the pre-monsoon season, the monsoon trough is north of Darwin, and southeasterly flow off the Australian continent at lower levels toward the monsoon trough places Darwin within a continental air mass. In this regime, intense afternoon heating generates deep isolated thunderstorms over the continent [*Rutledge et al.*, 1992]. Elevated topography to the east and southeast of Darwin, as well as Melville Island north of Darwin, are preferred regions for convective triggering. During the monsoon season, on the other hand, the monsoon trough reaches Darwin and moves inland to the south of Darwin, and northerly flow off the ocean at low levels is given a westerly component bringing maritime air to Darwin. In this regime, well-organized mesoscale cloud systems often occur with extensive stratiform cloud decks.

[16] Monthly average outgoing long-wave radiation (OLR) flux in December 2000 and its anomaly from the 30-year average (1970–2000) are shown in Figures 2a and 2b. As seen in these figures, a band with high-altitude clouds (low OLR flux) extended from the South Pacific Convergence Zone (SPCZ) to northern Australia along a longitude line of 140°E. A corresponding anomaly appeared over northern Australia, as a result of the earlier-than-average onset of monsoonal flow and convection. Because of these meteorological conditions, we could not find isolated deep convection in the northern Australian region. We therefore made measurements downstream of convective activity in cloud clusters in association with the monsoon trough and/or cyclone, as described in detail in the next section.

[17] A time series of the daily number of GPATS-detected lightning flashes in the region within 10–20°S and 125–145°E is shown in Figure 3. As seen in this figure, lightning activity during the BIBLE-C experiment was lower than that in early November, in accordance with the fact that lightning activity in northern Australia is generally greater during the pre-monsoon period as compared to the monsoon period.

4. Results and Discussion

4.1. General Features in the Study Area

[18] In this study, an area was chosen between 12–18°S and 129–138°E, in which most of the measurements from Darwin were made (Figure 1). Data obtained within this study area are shown and examined in this section after removing data that were obtained near the airport during take off and landing. These data were obtained during 10 local flights, which were made between November 30 and December 14, 2000. Vertical profiles of CO, NO_x, NO_y, and NO_x/NO_y, obtained within the study area are shown in Figure 4. In these figures, data obtained during flights 10 and 13 are shown using red and blue color coding, respectively. As seen in this figure, sharp enhancements of NO_x and NO_y were observed at altitudes between 11.5 and 14 km during flights 10 and 13. A lack of a corresponding increase in CO at these altitudes indicates that these enhancements were not primarily due to the vertical transport of air parcels which had been influenced by fossil fuel combustion and biomass burning near the ground. In fact, when NO_x mixing ratio is plotted versus CO mixing ratio (Figure 5), no correlation is found in air masses sample between 11.5–14 km. Further more, no clear correlation is found between NO_x and C_2H_2 and between NO_x and CH_3Cl, confirming negligible influences from fossil fuel combustion or biomass burning (not shown). Considering the very light air traffic around Darwin, the enhancements were quite likely due to recent lightning NO production. Because of the clear signatures of lightning NO production observed during flights 10 and 13, these two cases are examined in detail in this study.

[19] The CO data obtained at altitudes between 10 and 14 km in the study area can be classified into two groups with distinct differences in their CO mixing ratios (Figure 4). The CO mixing ratios obtained during flights 10 and 13 belong to the group with higher values and they generally increased with altitude. These features are probably because convection, which caused lightning, brought air parcels from near the surface to the middle and upper troposphere, although it likely had a small effect on NO_x levels as described above. As we will see in the next section, air masses sampled at 11.5–14 km during both flights 10 and 13 were quite likely affected by convection over land near the coast of the Gulf of Carpentaria. On the other hand, air parcels that had not been affected by convection sampled during other flights were generally transported from over the Central Pacific by easterly winds. It is therefore reasonable that CO levels in

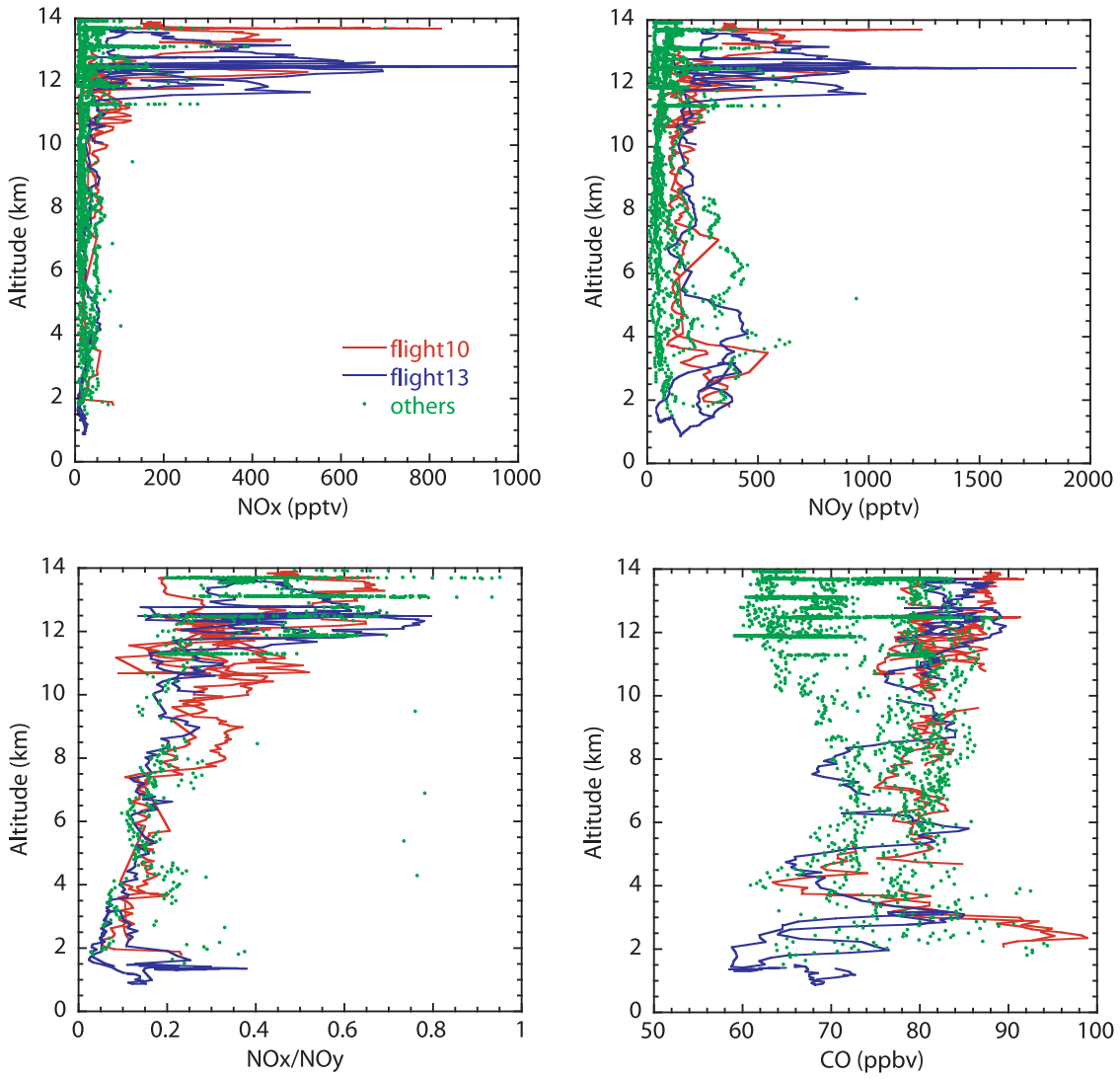

Figure 4. Vertical profiles of NO_x, NO_y, NO_x/NO_y, and CO mixing ratios observed in the study area, which was chosen as shown in Figure 1 (10-s data). Data obtained during flights 10 and 13 are shown using red and blue lines, respectively.

air parcels influenced by convection near the land were generally higher as compared to those in these pristine air parcels that originated from the Central Pacific. A similar positive correlation in lightning events was also reported based on measurements near Indonesia [*Koike et al.*, 2002a].

[20] The NO_x/NO_y ratios were about 0.6 and 0.8 when enhancements of NO_x and NO_y were observed during flights 10 and 13, respectively. The ratios were lower than unity suggesting that NO_y species other than NO_x, such as HNO_3 and PAN had been transported from the lower troposphere, although HNO_3 had likely been removed efficiently by wet deposition within the convection system. From the relationship between observed NO_x and NO_y mixing ratios, the contribution of lower tropospheric species other than NO_x is estimated to be about 200 pptv to the observed NO_y levels. Contributions from the lower troposphere are discussed further in section 4.4.

4.2. Flight 10 on 001209

4.2.1. General Features

[21] Flight 10 was made from Darwin and measurements at altitudes above 10 km were made between 0:00 and 03:20 on December 9 (UT). The flight track and lightning flash activity that had occurred within 24 h prior to the measurements are shown in Figure 6. In this figure, the NO_x mixing ratio observed onboard the aircraft is also shown using color coding along the flight track. Lightning occurred in the area where measurements were made, namely near the coast of the Gulf of Carpentaria about 14 h before, at around 10:00–14:00 on December 8. The activity gradually moved northeastwardly, and most of the lightning occurred over Gulf of Carpentaria after 14:00 on December 8. Streamlines and the horizontal wind speed at 200 hPa (about 12.5 km) at 0:00 UT on December 9, when measurements above 10 km started, are shown in Figure 7 using European Centre for Medium-Range Weather Forecasts (ECMWF) 1° × 1°

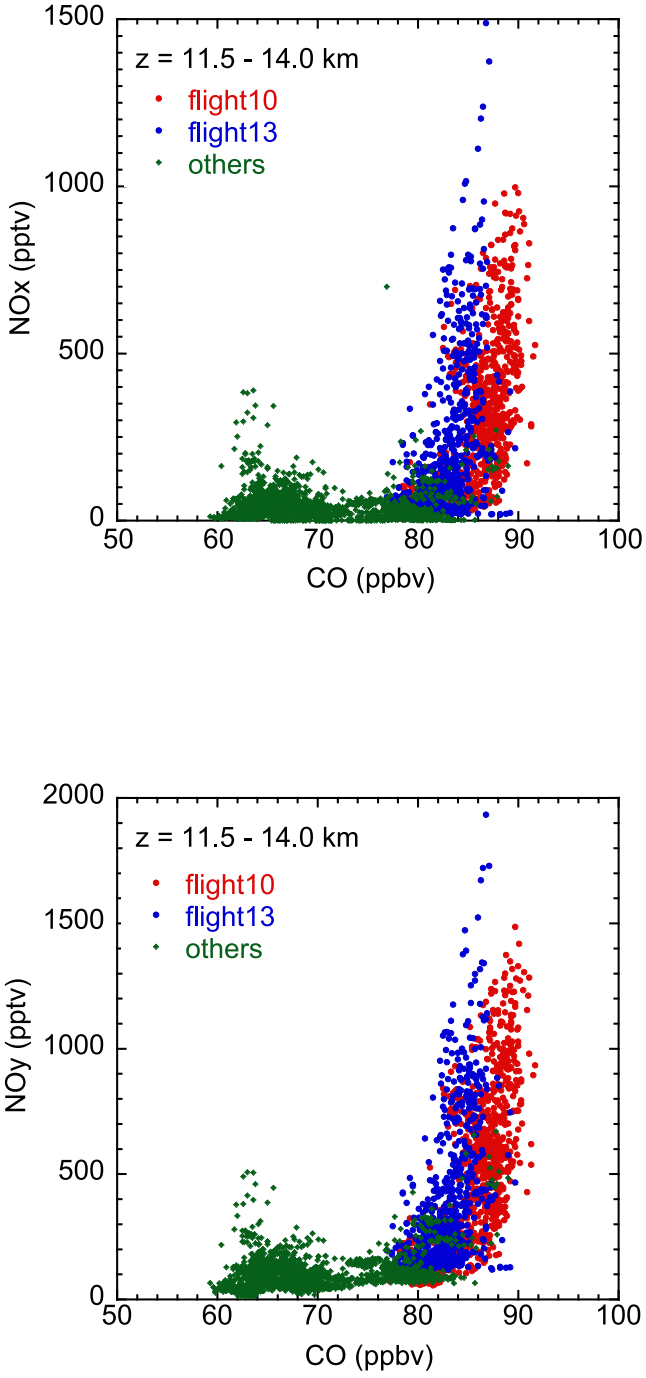

Figure 5. Scatterplots between NO_x and CO and between NO_y and CO obtained at altitudes between 11.5 and 14 km within the study area, which was chosen as shown in Figure 1. Data obtained during flights 10 and 13 are shown using red and blue circles, respectively.

data. As seen in this figure, easterly winds generally dominated over the study area, suggesting that the observed high NO_x mixing ratios were due to lightning activity that occurred over the coast of the Gulf of Carpentaria. As described in section 4.2.4, forward trajectories of air parcels influenced by lightning further confirm this. Further analyses on lightning data and five-day back trajectories starting from this lightning event show that prior to this lightning event (10:00–14:00 on December 8), air parcels had been transported from over Gulf of Carpentaria and are not considered to have been influenced by upwind lightning events and midlatitude air.

4.2.2. Aircraft Data

[22] Time series of NO_x, NO_y, NO_x/NO_y, CO, H_2O, wind speed, and wind direction are shown in Figure 8. As seen in this figure, NO_x mixing ratios between 400 and 1000 pptv were observed during three time periods, around 0:20, 1:30, and 2:30. The NO_y mixing ratio reached 1000–1500 pptv, and the NO_x/NO_y ratio ranged over 0.5–0.7 within these three large NO_x enhancement events. All these high values were observed around the same location of 15–16°S and 134–135°E (Figure 6). The first two events were observed at 12.5 km, separated by one hour, while the last event was observed at 13.7 km another hour later. These persistent structures of NO_x enhancements are also confirmed in Figure 9 in which NO_x mixing ratios are shown as a function of longitude for four different legs (three at 12.5 km and one at 13.7 km). Note that the aircraft flew almost parallel to the local wind direction during these four legs (Figures 6 and 7). A similar longitudinal distribution of NO_x mixing ratios is seen for each of these legs, suggesting that enhancements with similar spatial structure extended for a distance of 140 km to the direction which is perpendicular to the local wind direction, and more than 1 km vertically. Along the wind direction, NO_x enhancements (>100 pptv) extended about 620 km. It is also seen in Figure 9 that the NO_x concentration generally decreased gradually around the maximum, suggesting that we successfully sampled air parcels most severely influenced by lightning in this region and covered the major area of influence from this lightning event, at least in the horizontal direction. The average mixing ratio (±one standard deviation) of this enhanced NO_x region (140 × 620 km) at altitudes between 11.5 and 14 km was 291 ± 224 pptv (median value is 272 pptv) (Table 2).

[23] Signatures of lightning NO production have been detected during various aircraft measurements at midlatitudes [e.g., *Lange et al.*, 2001; *Jeker et al.*, 2000; *Allen et al.*, 2000; *Huntrieser et al.*, 2002] and the tropics [e.g., *Kawakami et al.*, 1997; *Koike et al.*, 2002a]. For example, *Kawakami et al.* [1997] showed elevated levels of NO (50–300 pptv) and NO_y (100–450 pptv) extending about 400 km near New Guinea Island (5°S, 150°E) observed during the Pacific Exploratory Mission-West B (PEM West-B). In addition to active cloud clusters near the research aircraft, there was some lightning activity within stagnated air within 3 days prior to the measurements and the authors could not identify which events were responsible for the elevated NO and NO_y levels. At midlatitudes, an NO plume between 400 and 800 pptv extending about 1000 km was observed from an aircraft along the flight track during the Nitrogen Oxides and Ozone Along Air Routes (NOXAR) experiment [*Jeker et al.*, 2000]. These high NO values were attributed to lightning caused by a series of deep convection cells over the Atlantic Ocean. To our knowledge, it has never before been reported that a NO_x enhancement has extended over such a wide area as 140 × 620 km (perpendicular × parallel to the wind direction) as observed in this study due to a single thunderstorm system, at least in the tropics. Consid-

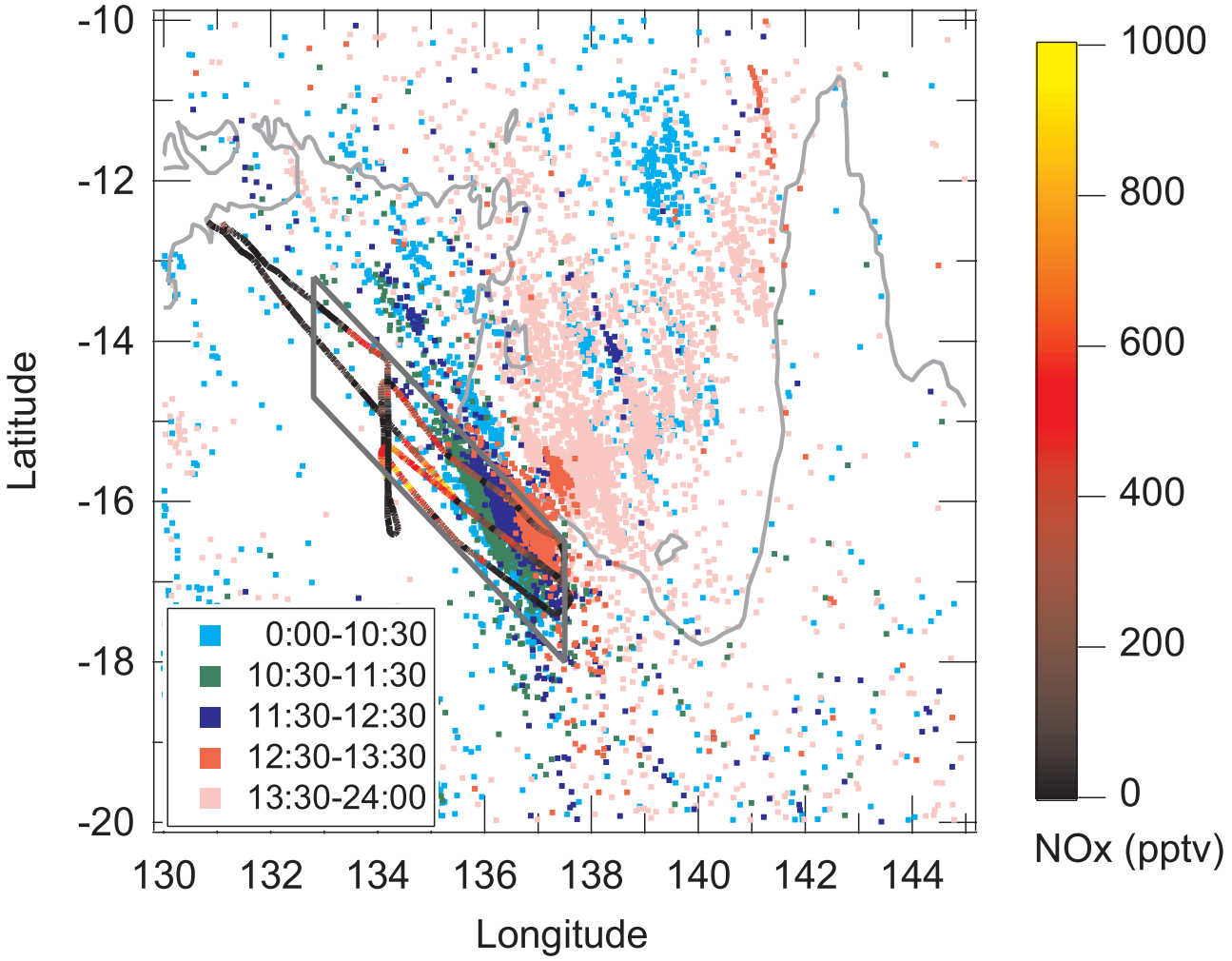

Figure 6. Flight track for the research aircraft for flight 10. Color coding of the flight track indicates NO_x mixing ratios at individual sampling points. Locations of flashes detected by the GPATS system are also shown using squares. Their color coding indicates the local time of flash events on December 8. Flight 10 measurements were made between 0:00 and 3:30 on December 9. The parallelogram shows the area in which air parcels influenced by lightning activity are assumed to have been transported. The area within the parallelogram corresponds to the area S in equation (3) in the estimate of the total NO amount produced by lightning.

ering the high frequency of such storm events in the tropics, lightning NO production should have a significant impact on reactive nitrogen levels there.

[24] On the other hand, NO_x and NO_y levels lower than 100 pptv were also occasionally observed, for example around 2:00 and 3:00 UT (Figure 8). Variability in NO_x and NO_y mixing ratios were also quite low in these air parcels. When air parcels with NO_y mixing ratios lower than 100 pptv were selected at 11.5–14 km, the average NO_x and NO_y (±one standard deviation) was found to be 15 ± 6 and 67 ± 16 pptv, respectively. These NO_x values were even slightly lower than the average in the study area of 41 ± 42 (at 11.5–14 km, excluding flight 10 and 13 data), suggesting that in these occasions we sampled background air masses, which had not been influenced by lightning around northern Australia. The CO levels were also low in these air masses, consistent with a lack of influence from convection over land.

[25] When a scatterplot is made between NO_x and H_2O mixing ratios, no correlation or very weak negative correlation is found at an altitude of 12.5 km (not shown). A negative correlation is more clearly seen between CO and H_2O mixing ratios (r = 0.50) and between O_3 and H_2O mixing ratios (r = 0.56). These negative correlations appear to be unexpected when the fact that convection brings water vapor, CO, and O_3 from lower altitudes is considered. A possible explanation is that during upward motion, air parcels in the convective systems overshot the expected cloud top altitude at which the temperature of air parcels becomes equal to that of ambient air. In these air parcels, the water vapor mixing ratio is considered to be lower due to precipitation as compared with that in ambient air with a relative humidity of 100% at the expected cloud top altitude. In fact, the relative humidity over ice was greater than 90% for 70% of the data at 12.5 km, and the CO and

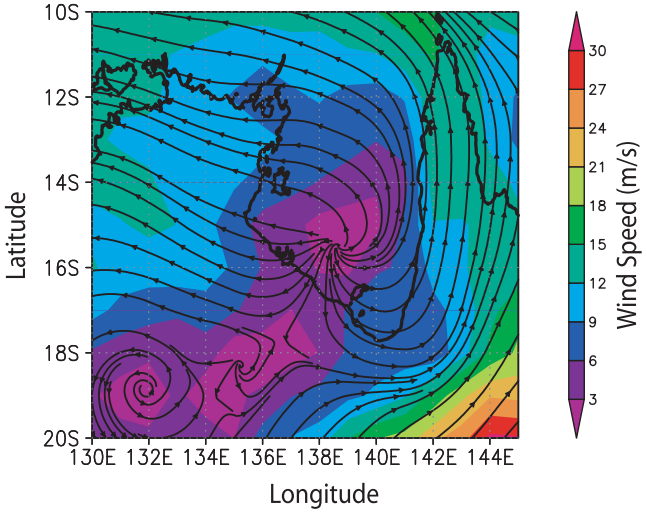

Figure 7. Streamlines (arrows) and wind speed (color contours) of horizontal winds at 200 hPa (about 12.5 km) at 00:00 UT on December 9, when flight 10 was conducted.

O_3 mixing ratios were systematically higher in lower humidity air (not shown).

[26] The wind speed observed on board the aircraft between 11.5–14 km (Figure 8) shows two distinct regimes; one with relatively low wind speeds of 1–4 m s^{-1} and another with high wind speeds of 16–22 m s^{-1}. ECMWF data at 200 hPa (about 12.5 km) at 0:00 UT (Figure 7) show that the wind speeds were 6–12 m s^{-1}. An easterly wind direction (110 ± 10°) is consistent between in-situ measurements and ECMWF data. These results suggest that ECMWF wind data were generally consistent with in-situ observations during the flight, although local cloud systems, such as divergent flow from clouds over the Gulf of Carpentaria, affected the local wind field over the study area.

4.2.3. Cloud System and Lightning Flashes

[27] In Figure 10, Geostationary Meteorological Satellite (GMS) cloud (brightness temperature) images are shown every hour between 9:00 and 14:00 UT on December 8. In this figure, the locations of GPATS-detected flashes, which were likely responsible for enhancements of NO_x observed during flight 10, are also shown. In this figure, we can see an evolution of a cloud system and corresponding lightning activity. Convective activity appeared near the coast of the Gulf of Carpentaria between 9:00 and 10:00 UT, and it intensified until 12:00 UT. A region with cloud top temperatures lower than 187 K (about 17 km), which is shown with the yellow-red color in Figure 10, extended to 190 × 120 km at 12:00 UT, and most of the lightning flashes were detected by GPATS in this region. The tropopause height and temperature were 17.3 km and 186 K, respectively, according to balloon-sonde data at Darwin at 11:00 UT, indicating that convection that was accompanied by lightning reached close to the tropopause altitude. The convective system moved northeastward after 12:00 UT with decreasing lightning intensity. A time series of lightning flash numbers detected by GPATS is shown in Figure 11. In accordance with the cloud activity shown in Figure 10, the number of lightning flashes increased from 9:00 UT, and high flash counts were observed between 10:00 and 13:00 UT.

[28] Figure 10 also shows that the locations of GPATS flashes generally agree with those of GMS-derived high altitude clouds. GPATS-derived lightning activity moved northeastward with the cloud system. By comparing the locations of high altitude clouds and GPATS-detected flashes, the accuracy of positioning by GPATS for this event has been estimated to be 60 ± 20 and 8 ± 2 km, in the northwest and northeast directions, respectively. The difference in positioning accuracies in the two directions is because the three receivers used to identify lightning locations are located southeast from the cloud system (open circles in Figure 1), and the error in positioning tends to become greater toward the gazing direction (northwest) as compared to the perpendicular direction (northeast). Consequently, although the locations of GPATS-detected light-

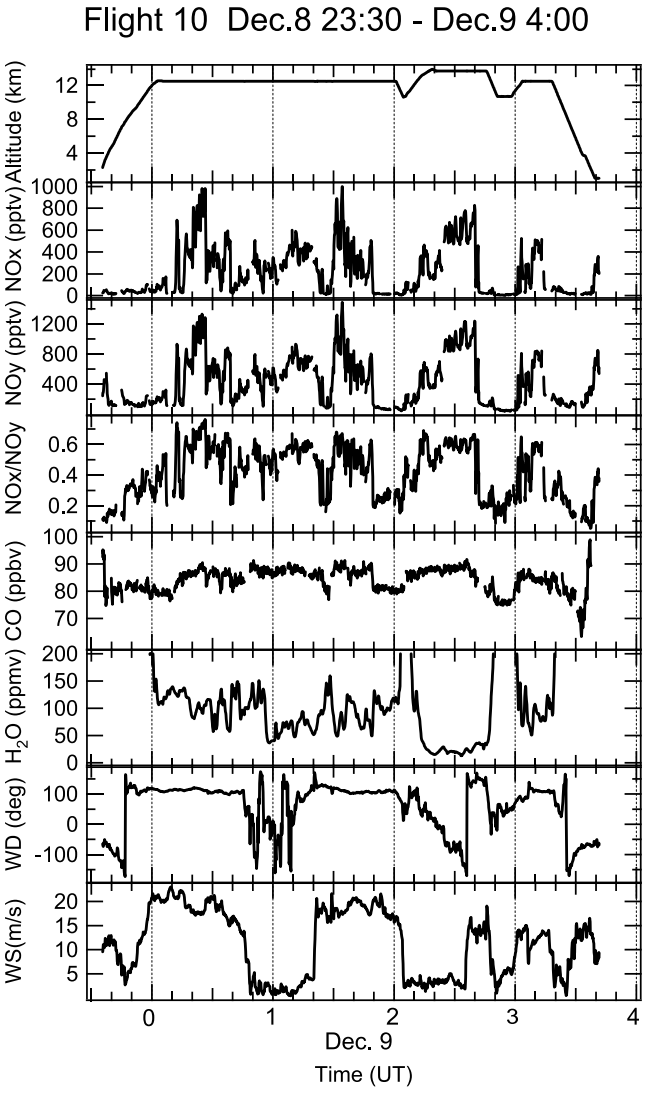

Figure 8. Time series of various parameters observed on board the aircraft during flight 10 (10-s data). WD and WS stand for wind direction and wind speed, respectively.

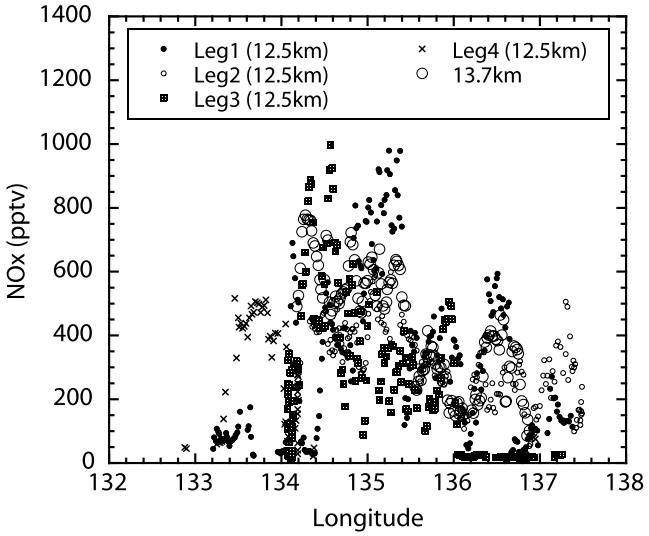

Figure 9. Longitudinal distribution of NO_x observed during flight 10. Different symbols are used for data obtained during 4 different legs made at 12.5 km and data obtained at 13.7 km. Within 3 transverse legs at 12.5 km between 134°E and 138°E (Figure 6), leg 1 is in the middle, and legs 2 and 3 are to the north and south of leg 1, respectively. Leg 4 was made on the way back to Darwin. The leg at 13.7 km was made along leg 1.

ning flashes stretched toward the northwest direction, this was partly due to an error in positioning.

[29] Radar echo intensity at altitudes around 3 km measured by the Bureau of Meteorology in Australia is also shown for 12:00 UT (Figure 12). Areas with radar echoes greater than 14 dBZ (precipitation rates of about 0.3–2 mm h^{-1}, shown with dark blue in Figure 12) generally correspond to locations where lightning flashes were detected by GPATS, and areas with 28–39 dBZ (2–10 mm h^{-1}, shown with light blue) correspond to locations where the highest number of flashes was detected. These results are generally consistent with previous studies [e.g., *Rutledge and MacGorman*, 1988; *Defer et al.*, 2001].

4.2.4. Forward Trajectories From Lightning Area

[30] As seen in Figure 6, intense lightning activity was detected near the flight track between 10:30 and 13:30 on December 8. Considering the wind field during the measurements (Figure 7), air influenced by this lightning activity is considered to have been transported to the flight track region by the time of measurements and was sampled onboard the aircraft. To confirm this point, forward trajectories of air parcels influenced by these lightning flashes between 11:00 and 13:00 UT, when most intense lightning activity was observed (Figure 11), were calculated. In Figure 13 locations of air parcels at 00:00 UT on December 9, when we observed high NO_x air (Figure 8) are shown. In these calculations, ECMWF data (the 6-hourly data with 1° resolution in latitude and longitude) and a method described by *Tomikawa and Sato* [2005] were used. Trajectories were calculated from an altitude of 12 km. The total number of lightning flashes that affected individual air parcels is color-coded. Strictly speaking, the total flash number was summed within a column of air at the end point of the trajectories, because air parcels had arrived at different altitudes. Because of higher wind speed at higher altitudes, air parcels transported to higher altitudes reached further northwestward as compared with those transported at lower altitudes. As can be seen in this figure, locations at which enhanced levels of NO_x were observed are generally consistent with these trajectories of air influenced by lightning flashes. This result further confirms that observed NO_x enhancements were due to lightning activity between

Table 2. Summary of Flight 10 and 13 Events

Flight	Flight 10		Flight 13	
NO_x average (pptv in 11.5–14 km)	291 ± 215		209 ± 225	
$(NO_x)_{LT}$ (pptv)[a]	28 ± 14		28 ± 14	
Area of high-NO_x air, km^2[b]	8.50×10^4		6.66×10^4	
Altitude range of high-NO_x air, km	11.5–14.0		11.5–14.0	
Total number of NO_x molecules produced by lightning (11.5–14 km)[c]	3.28×10^{29}		1.79×10^{29}	
Total number of NO_x molecules produced by lightning (0–16 km)[d]	10.8×10^{29}		5.87×10^{29}	
GPATS flash counts	3260		402	
Estimated CG flash counts[e]	3260	1410	402	171
Estimated total flash counts[f]	57,400	24,900	2750	1170
NO production rate (molecules/flash between 11.5–14 km)[c]	0.571×10^{25}	1.32×10^{25}	6.51×10^{25}	15.3×10^{25}
NO production rate (molecules/flash between 0–16 km)[d]	1.88×10^{25}	4.35×10^{25}	21.0×10^{25}	49.3×10^{25}
Global NO production rate (0–16 km) (Tg(N)/yr)[g]	0.619	1.43	6.93	16.3

[a]Estimated contribution of vertically transported lower-tropospheric NO_x (section 4.4).

[b]Area in which high-NO_x air (defined as NO_x > 100 pptv) is considered to be distributed (Figures 6 and 14; section 4.5).

[c]Calculated using equation (3). The range of 11.5–14 km is the observed range of high-NO_x air; however, we assumed in this paper that these air parcels were located at the same altitude range when they had left the thunderstorm (section 4.6).

[d]These estimates are derived by multiplying the produced NO_x amounts between 11.5 and 14 km by a factor of 3.2 using the results reported by *Pickering et al.* [1998] (section 4.6).

[e]Greater values are derived by assuming that all the GPATS-detected lightning flashes are CG flashes. Smaller values are derived by assuming that 60% of positive flashes detected by GPATS are IC flashes. See the text for details (sections 2.2 and 4.7).

[f]Total lightning flash number ($N_{IC} + N_{CG}$) was estimated from the CG flash number and empirical parameterization developed by *Price and Rind* [1993] (equation (4), section 4.7).

[g]The global lightning flash frequency of 44 flashes s^{-1} [*Christian et al.*, 2003] is used (section 4.7).

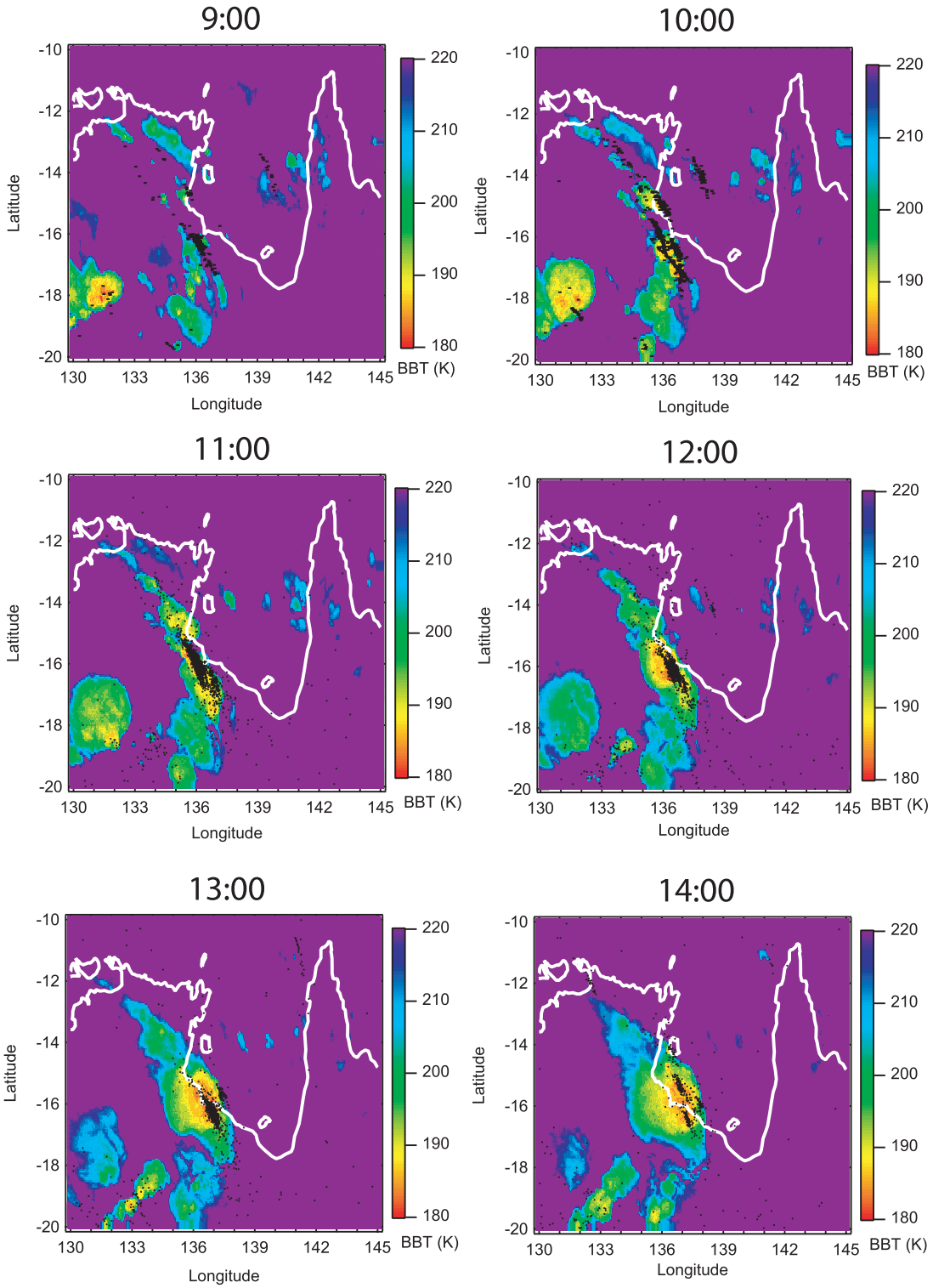

Figure 10. GMS cloud height images (color contours) and locations of GPATS-detected flashes (closed circles) between 9:00 and 14:00 UT on December 8. For GPATS data, those obtained for each one-h period are plotted (for example, with GMS cloud image at 9:00, GPATS data obtained between 8:30 and 9:30 are plotted).

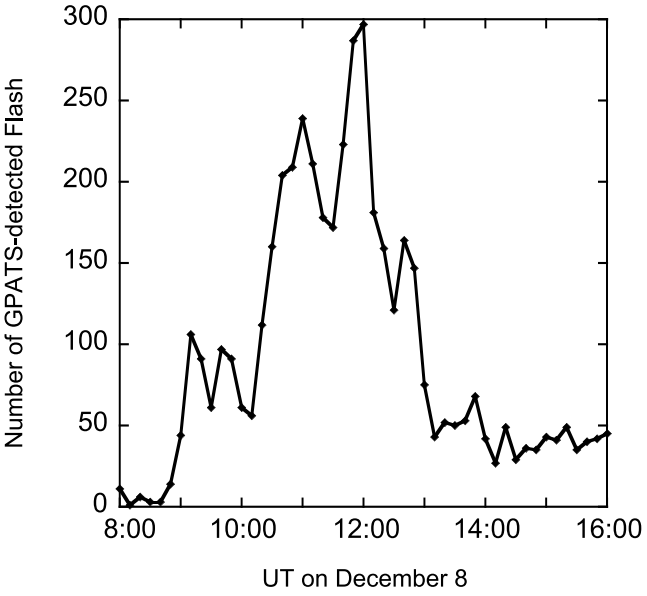

Figure 11. GPATS-detected lightning flash counts every 10 min in the area within 13–18°S and 132–140°E.

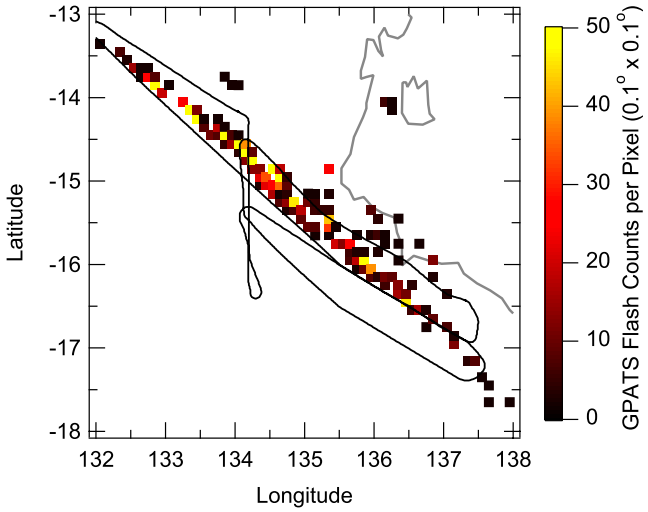

Figure 13. Locations of air parcels at 00:00 UT on December 9, which were influenced by GPATS-detected lightning flashes between 11:00 and 13:00 UT on December 8. Forward trajectories of air parcels were calculated from locations of GPATS lightning flashes (every pixel of 0.1° × 0.1° in latitude and longitude) and an altitude of 12 km using ECMWF data. Color coding shows the number of GPATS lightning flashes that affected individual air parcels (0.1° × 0.1° pixel).

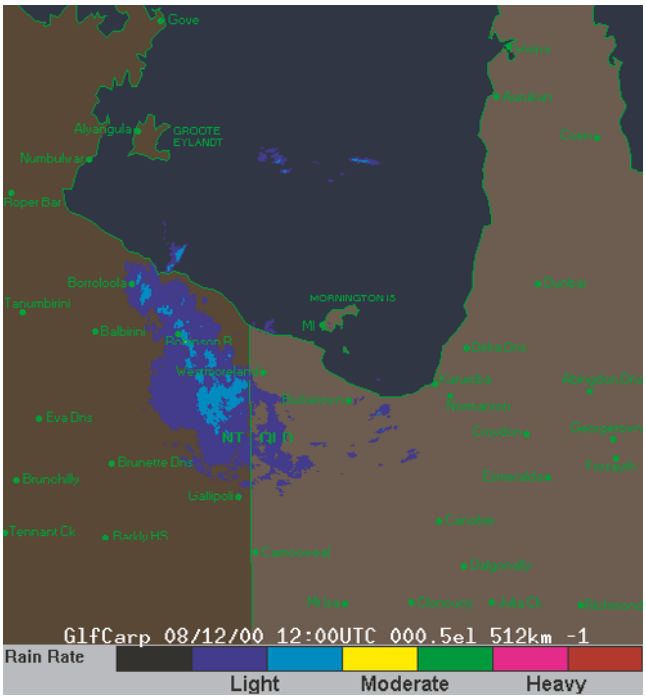

Figure 12. Radar echo measured by the Bureau of Meteorology in Australia at 0:00 UT on December 8. Color ranges are 14–28 dBZ (corresponding to precipitation of 0.3–2 mm h^{-1}, when the Marshall-Palmer raindrop size distribution [*Marshall and Palmer*, 1948] is assumed, dark blue), 28–39 dBZ (2–10 mm h^{-1}, light blue), 39–44 dBZ (10–20 mm h^{-1}, yellow), 44–48 dBZ (20–40 mm h^{-1}, green), 48–55 dBZ (40–100 mm h^{-1}, pink), and >55 dBZ (>100 mm h^{-1}, red).

10:00 and 14:00 UT and our aircraft measurements successfully covered the area in which high NO_x air had spread.

4.3. Flight 13 on 001211–001212

[31] Flight 13 was made from Darwin and measurements at altitudes between 11 and 14 km were made between 22:10 UT on December 11 and 00:40 on December 12 UT (Figures 14 and 15). During this flight NO_x and NO_y mixing ratios as high as 1500 and 2000 pptv were observed over the Arnhem Land Peninsula. Back trajectory calculations and GPATS measurements suggest that these high NO_x values were likely due to NO production by lightning on the east coast of the Arnhem Land Peninsula to the Gulf of Carpentaria between 13:00 and 15:00 UT on December 11 (10–12 h prior to the measurements). As can be seen in Figure 14, we successfully sampled air in the area around the location where the highest NO_x mixing ratios were observed. The area of high NO_x air (>100 pptv) extended 400 and 170 km along and perpendicular to the wind direction, respectively, in which the average (± one standard deviation) of NO_x mixing ratio was 209 ± 225 pptv (the median value was 114 pptv) at altitudes between 11.5 and 14 km (Table 2). Although this area is 2/3 of that observed during flight 10, enhancements of NO_x covering such a large area due to a single thunderstorm system in the tropics have never been reported before.

[32] In Figure 16 the locations of lightning flashes detected by the GPATS system overlaid on GMS cloud height images are shown for every hour between 12:00 and 15:00 UT on December 11. Note that for this figure a color-scale different from that used for flight 10 (Figure 10) is used. For the case of flight 10, intense lightning activity was

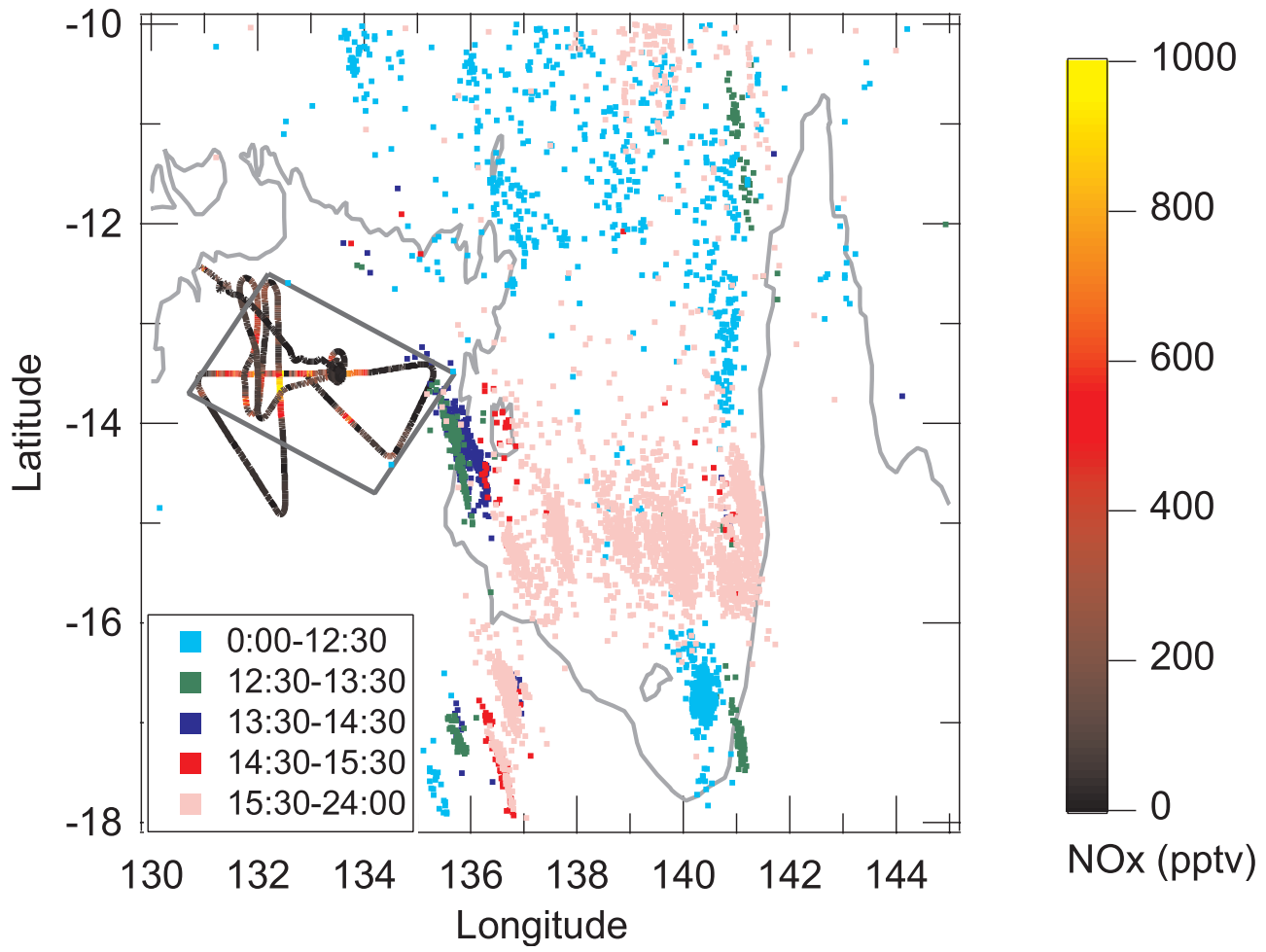

Figure 14. Flight track for the research aircraft for flight 13. Color coding of the flight track indicates NO_x mixing ratios at individual sampling points. Locations of flashes detected by GPATS system are also shown using squares. Their color coding indicates the local time of flash events on December 11. Flight 13 measurements were made between 22:10 UT on December 11 and 00:40 on December 12. A parallelogram shows the area in which air parcels influenced by lightning activity are assumed to have been transported. The area within the parallelogram corresponds to area S in equation (3) in the estimate of the total NO amount produced by lightning.

detected when convection (high altitude cloud) was observed from the GMS satellite. For the case of flight 13, however, the area of high altitude clouds (cloud top temperature <190 K, about 16 km), which appeared on the east side of the Arnhem Land Peninsula at 14:00 UT, was quite limited (Figure 16). In accordance with this less pronounced convective activity as compared with that of the flight 10 thunderstorm, the number of lightning flashes detected by GPATS between 12:00 and 15:00 UT was only 402, which is a factor of 8 smaller than the 3260 of flight 10. Radar echo image obtained by the Australian Bureau of Meteorology at 13:40 on December 11 is shown in Figure 17. Although areas with radar echoes greater than 14–39 dBZ (dark and light blue in Figure 17) generally correspond to locations where lightning flashes were detected by GPATS as for the case of flight 10 (Figure 12), the area is much smaller as compared to the case for flight 10.

4.4. Influences From Vertical Transport of Lower-Tropospheric Air

[33] As described in section 4.1, a part of the reactive nitrogen species observed in the middle and upper troposphere is considered to have been vertically transported by convection from the lower troposphere, where these species are emitted from anthropogenic combustion sources and probably from soil. To evaluate the influences from these sources, a correlation of NO_x and NO_y with CO in the lower troposphere is examined, because CO is a good tracer of influences from combustion sources and, in general, influences from lower-tropospheric air. During flights 10 and 13 in which significant enhancements in NO_x and NO_y were observed, air parcels underneath the convection systems were not sampled. Consequently, average NO_x-CO and NO_y-CO relationships obtained in the lower troposphere in the study area, which covers the Arnhem Land Peninsula (Figure 1), are used in this study. This is partly justified by

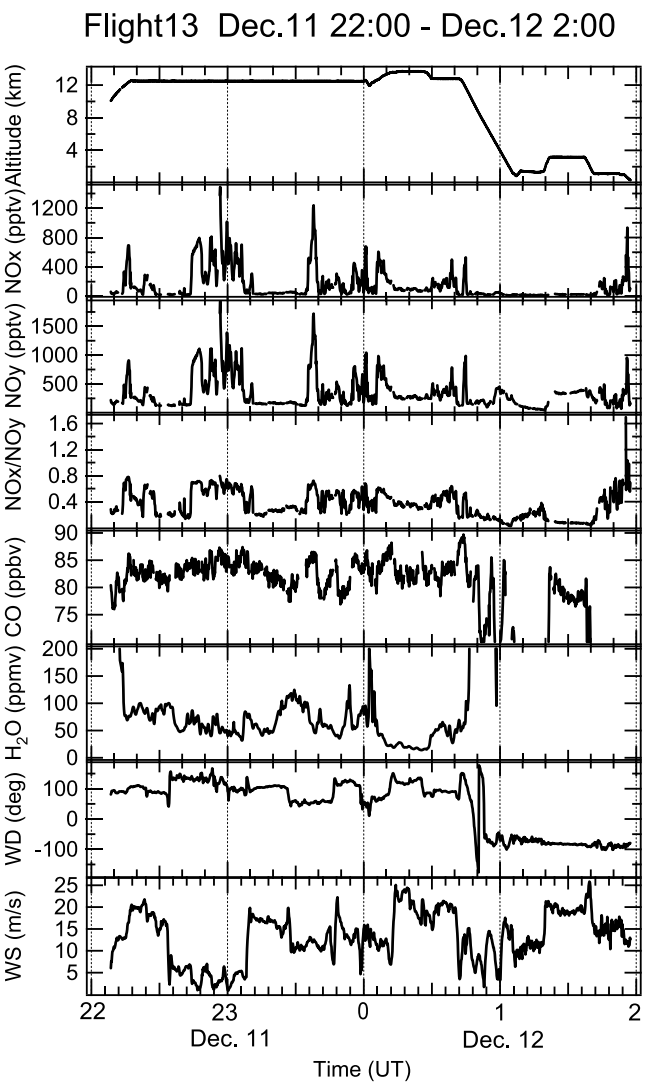

Figure 15. Time series of various parameters observed on board the aircraft during flight 13 (10-s data). WD and WS stand for wind direction and wind speed, respectively.

the fact that lower-tropospheric air in the flight 10 and 13 convection systems were generally transported from over the Arnhem Land Peninsula by westerlies, according to back trajectory analyses (not shown).

[34] As shown in Figure 4, increases in CO mixing ratios were observed at altitudes below 4 km, however, no clear correlation is found between NO_x and CO mixing ratios in this altitude range (not shown). A range of CO mixing ratios, 80 to 95 ppbv, was observed during flights 10 and 13 at altitudes between 11.5 and 14 km. An average NO_x mixing ratio of 28 ± 14 pptv (1-σ) for air within this CO range at altitudes below 4 km is used to subtract the contribution of transport of lower-tropospheric air, assuming that background values of CO and NO_x are the same between these two altitude ranges (Table 2). Similarly, an average NO_y mixing ratio of 252 ± 145 pptv was obtained for the influence of lower-tropospheric air. This estimate is generally consistent with the estimate of 200 pptv (NO_y species other than NO_x) derived from a deviation of the NO_x/NO_y ratio from unity, described in section 4.1.

4.5. Estimates of Total NO Amount Produced by Thunderstorm

[35] In this study, the NO production rate by lightning (number of NO molecules produced by a single lightning flash) is estimated using NO_x data. In this section the total amount of NO produced by each lightning event is shown. An estimate can also be derived using NO_y data; however, the uncertainty is greater due to the greater influences from lower-tropospheric air. Loss of NO_x by reaction with OH - following lightning NO production along trajectories by the time of aircraft observation - is estimated using the box model described in section 2.1. As a result, it is found to be negligible (2% and 0.5% for flights 10 and 13 data, respectively) and no correction is applied to the observed NO_x values in this study.

[36] Because the method used to estimate the NO production rate is the same for each flight, we describe the approach for flight 10, and only the results are given for flight 13. In this study, the NO production rate P (molecules by a single flash) was estimated by the following equation,

$$P = \frac{S \cdot \Delta z \cdot \left([NO_x] - [NO_x]_{LT}\right)}{N_{IC} + N_{CG}} \quad (3)$$

where S is the area in which air parcels influenced by lightning activity are transported, Δz is its vertical extent, $[NO_x]$ is the average NO_x concentration within a volume of $S\ \Delta z$, $[NO_x]_{LT}$ is the NO_x concentration transported from the lower troposphere (section 4.4), and $N_{IC} + N_{CG}$ is the number of lightning flashes.

[37] In this section, an estimate for the total NO amount, which is the numerator of the right hand side term of equation (3), is given. In Figure 6, the area in which air parcels influenced by lightning activity are considered to have been transported (NO_x > 100 pptv) is shown for flight 10. The value of 100 pptv is well above the back ground NO_x concentration (15 ± 6 pptv, section 4.2.2) and the lower tropospheric NO_x concentration (28 ± 14 pptv). The area (S in equation (3)) is calculated to be about 8.5×10^4 km^2 (Table 2). For the vertical extent (Δz in equation (3)), we only consider altitudes between 11.5 and 14 km, where enhancements of NO_x were observed. Possible influences above and below these altitudes are discussed in the next section. The average (± one standard deviation) of NO_x mixing ratio at 11.5–14 km is 291 ± 224 pptv (the median value is 272 pptv) for flight 10, and the NO_x value in air transported from the LT is estimated to be 28 ± 14 pptv (the median value is 26 pptv) (section 4.4). Using these values, we estimated the total number of NO_x molecules observed in the altitude range between 11.5 and 14 km produced by this thunderstorm to be 3.3×10^{29} (Tables 1 and 2). The total numbers of NO molecules produced from a single thunderstorm estimated in previous studies are summarized in Table 1. As can be seen in this table, the total NO amount for the flight 10 event is greater than that estimated for the moderately active storm observed during CRYSTAL-FACE (July 16) [*Ridley et al.*, 2004] and for storms observed during LINOX [*Huntrieser et al.*, 1998] and EULINOX [*Huntrieser et al.*, 2002]. It is as large as that estimated for

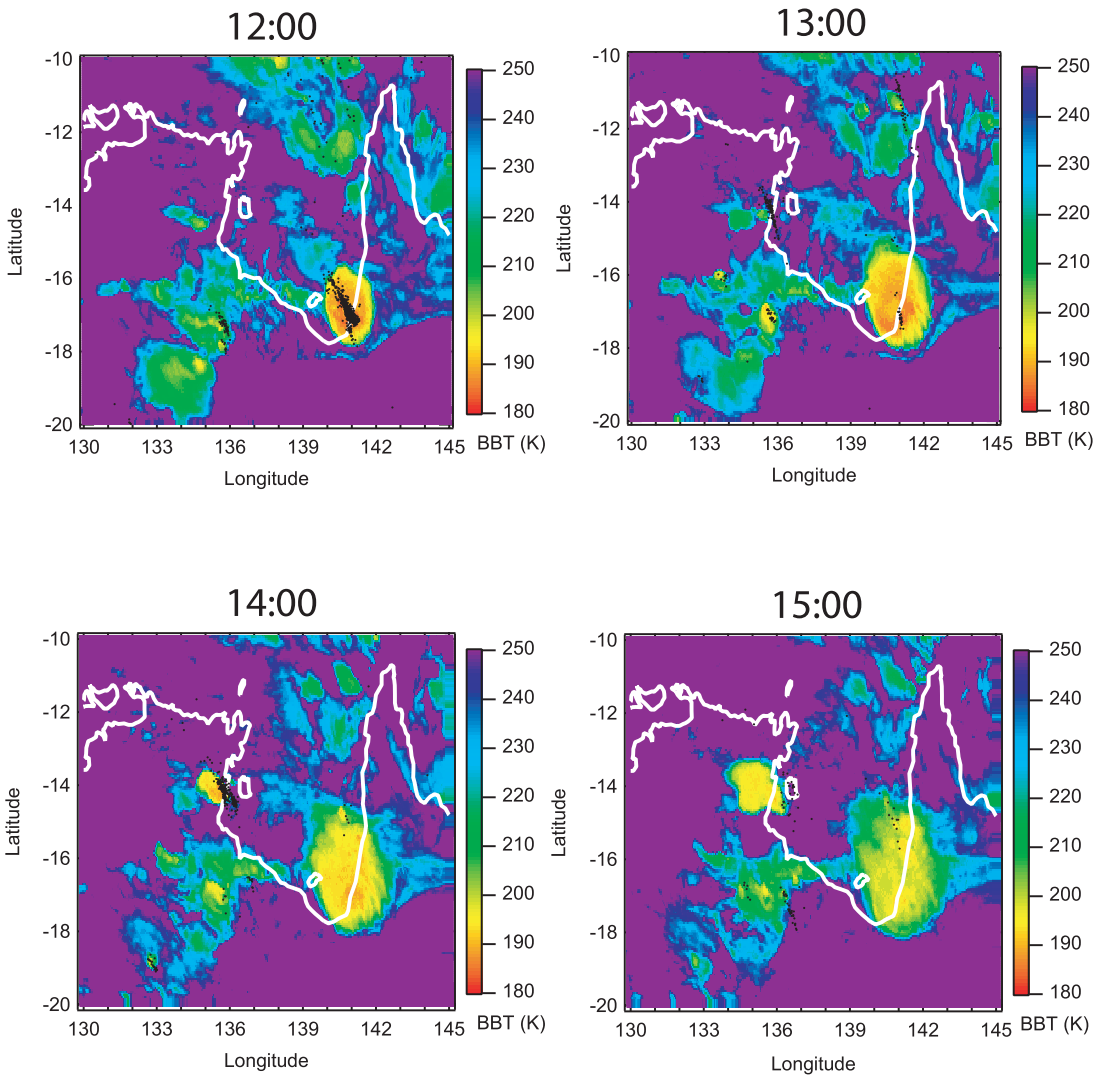

Figure 16. GMS cloud height images (color contours) and locations of GPATS-detected flashes (closed circles) between 12:00 and 15:00 UT on December 11. For GPATS data, those obtained for each one-h period are plotted (for example, with GMS cloud image at 12:00, GPATS data obtained between 11:30 and 12:30 are plotted). Although some lightning flashes are shown on the east coast of Arnhem Land Peninsula where there is low cloud activity for 13:00, these lightning flashes took place between 13:00 and 13:30 after this cloud image was obtained. Note that the color code used for this figure is different from one used for Figure 10 (Flight 10).

STERAO-A (July 10) [*Dye et al.*, 2000], although a far greater NO production event was also observed at midlatitudes during CRYSTAL-FACE (July 29) [*Ridley et al.*, 2004].

[38] The difference in the estimates between previous studies and this study is that enhanced NO_x levels were observed within an anvil of existing cloud systems in previous studies [e.g., *Ridley et al.*, 1996, 2004; *Huntrieser et al.*, 1998, 2002; *Dye et al.*, 2000; *Skamarock et al.*, 2003], while we observed enhanced NO_x values after the cloud system had completely dissipated. As a result, there are great uncertainties in estimating the influenced area S in equation (3), and the error can be as large as a factor of 2 in the estimate of the total NO production amount. This estimate was derived by examining the variability in wind speed and direction observed onboard the aircraft (section 4.2.2) and assuming a similar variability during the transport of air after the thunderstorm event.

[39] The total NO amount produced is also estimated for flight 13 in the same way as for flight 10. The area of lightning influence is shown in Figure 14 and it (S in equation (3)) is calculated to be about 6.7×10^4 km^2 (Table 2). The average NO_x mixing ratio at 11.5–14 km is 209 ± 225 pptv (median value is 114 pptv). Using the same lower-tropospheric NO_x value of 28 pptv, the total number of NO molecules produced by this lightning event is 1.8×10^{29} for the altitude range between 11.5 and 14 km (Tables 1 and 2). This value is about 60% of the flight 10 value and is still comparable with that of the STERAO-A July 10 case.

4.6. Altitude Extent of Lightning Influence

[40] Our estimates of the total NO production amount described in the previous section are limited to the altitudes

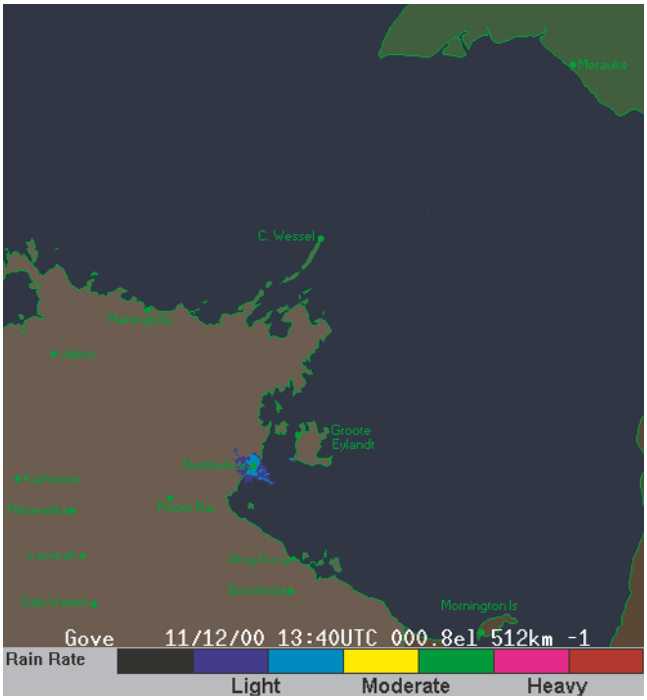

Figure 17. Radar echo measured by the Bureau of Meteorology in Australia at 13:40 UT on December 11. Color coding is same as for Figure 12.

between 11.5 and 14 km where high-NO_x air was observed. In this section, possible influences above and below this altitude range are discussed.

[41] As shown in Figure 4, enhancements of NO_x exceeding 400 pptv were observed only at altitudes above 11.5 or 12 km during flights 10 and 13, although increases up to 130 pptv were also observed at altitudes above 10.5 km during flight 10. In Figure 18, vertical profiles of wind speed and wind direction data obtained every 12 h by regular balloon-soundings at Darwin by the Australian Bureau of Meteorology are shown for the time period between 23:00 UT on December 7 and 11:00 UT on December 9. As clearly seen in this figure, there was a persistent wind shear at altitudes between 8 and 9 km; air parcels at altitudes above this altitude range were generally advected from the lightning region to the aircraft measurement region by easterlies, although there was some variability in wind direction (between 70 and 140 degrees). On the other hand, air parcels below this altitude range came from over the Timor Sea by westerlies, and they had not been influenced by lightning activity over the Gulf of Carpentaria. Wind data obtained on-board the aircraft and trajectory calculations using ECMWF data are generally consistent with these balloon-derived wind data. Consequently, it is very difficult to judge the reason for little or no enhancement in NO_x at altitudes below 11.5 km. It could be due to the wind shear or to the fact that most NO molecules produced by lightning had been transported to altitudes above 11.5 km within thunderclouds. Very small increases at altitudes between the wind shear altitude (6–9 km) and 11.5 km may suggest that an enhancement of NO_x was limited to altitudes above 11.5 km within the thunderclouds for this event.

[42] Because our measurements are limited to altitudes below 14 km, which is the upper altitude limit of the

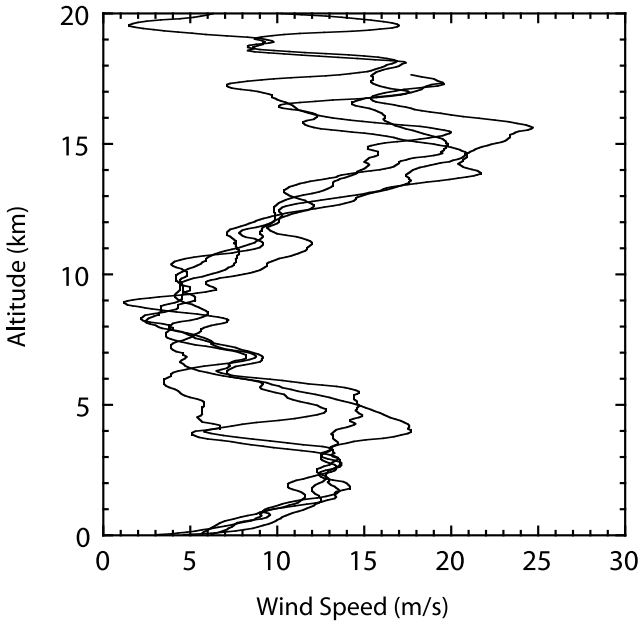

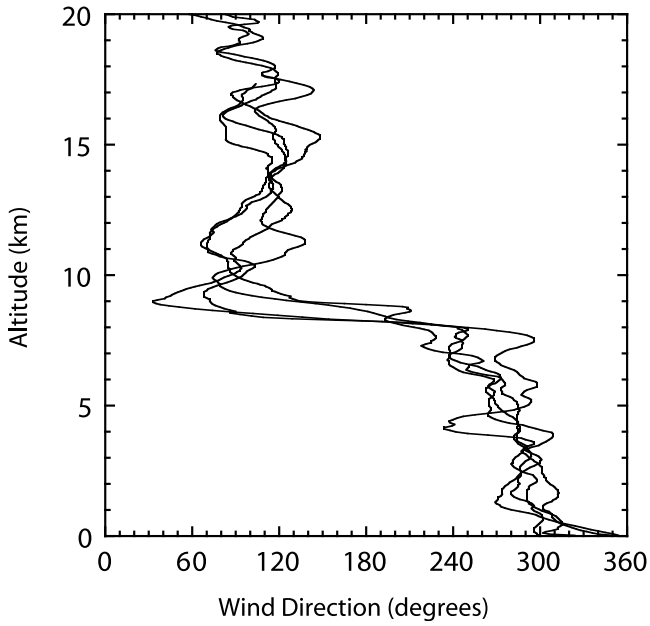

Figure 18. Vertical profiles of wind speed and wind direction observed at Darwin between 23:00 UT on December 7 and 11:00 UT on December 9 (every 12 h) by the Australian Bureau of Meteorology. Note that flight 10 was made on December 9 (00:00–03:00 UT) and lightning events for this flight took place on December 8 (10:00–14:00).

research aircraft used, we do not know the vertical extent of the influence from lightning above 14 km. For the case of flight 10, cloud top brightness temperatures obtained by the GMS satellite show that the highest altitude of the cloud systems was about 185 K (Figure 10), which corresponds to a tropopause temperature at about 17 km based on balloon-sounding data at Darwin. Back trajectories for sampled air parcels at 14 km were also examined, and the top altitudes of clouds at the location and time when trajectories had encountered clouds (see *Koike et al.* [2002a] and *Oshima et al.* [2004] for this method) were found to be between 14 and 16 km (190 and 208 K). These results indicate that NO production by lightning could have extended up to 16–17 km.

[43] The trajectory calculations show that changes in altitude of air parcels during transport from the thunderstorm to the points of measurement were less than 1 km, and therefore we assume that air parcels observed at altitudes between 11.5 and 14 km had been located at the same altitude range when they had left the thunderstorm. *Pickering et al.* [1998] estimated the vertical profile of lightning-generated NO_x mass distribution at the end of a thunderstorm using a two-dimensional cloud-resolving model with parameterizations of flash rate, flash type, flash location, and NO production rate. According to their study, the NO_x mass distribution for tropical continental storms with a top altitude of 16 km is 59, 31, and 10% at altitude ranges 0–11.5, 11.5–14, and 14–16 km, respectively. Because of the very small observed enhancements of NO_x below 11.5 km in our cases, the estimate for the 0–11.5 km range by *Pickering et al.* [1998] could be overestimated. On the other hand, the fraction at 14–16 (or 14–17) km can be greater than this estimate, and therefore the fraction at 11.5 and 14 km could be either greater or smaller than this estimate. If we simply use the faction of 31% estimated by *Pickering et al.* [1998], the total column NO production amount between 0 and 16 km will be 3.2 times greater than the estimate for the 11.5–14 km range and will be 11 and 5.9×10^{29} molecules for flight 10 and 13 case, respectively (Table 2). We estimated that this simple application can introduce an additional uncertainty of a factor of 1.5 to the column NO_x production amount, by examining a case in which NO_x production between 8 and 11.5 km is assumed to be zero or NO_x production between 14 and 17 km is assumed to be same as that between 11.5 and 14 km.

4.7. NO Production Rate

[44] In this section, the NO production rate (number of NO molecules produced by a single lightning flash) is estimated using equation (3). As described in section 2.2 and Appendix A, there is a possibility that a part of the IC flashes detected by the Australian GPATS during BIBLE-C was mislabeled as CG flashes. Therefore in this study we provide two estimates to study a range of uncertainties. In the first estimate we use GPATS-detected lightning flashes as CG flashes and in the second estimate we assume a part of GPATS flashes (60% of positive flashes) were in fact IC flashes.

[45] In both the estimates, we need to estimate the IC flash number from the CG flash number to obtain a total flash number ($N_{IC} + N_{CG}$). For this purpose, we used an empirical parameterization of the N_{IC}/N_{CG} ratio developed by *Price and Rind* [1993], which has been widely used for model calculations. In this parameterization, the ratio is expressed by a polynomial of the cold cloud thickness, which is defined by the thickness between the cloud top and the altitude of the 0°C isotherm in the cloud ($dz = z_{top} - z_{0°C}$, in units of km):

$$N_{IC}/N_{CG} = A\ dz^4 + B\ dz^3 + C\ dz^2 + D\ dz + E \qquad (4)$$

where A = 0.021, B = −0.648, C = 7.493, D = −36.54, E = 63.09 for a dz range between 5.5 and 14 km. This parameterization generally captures the features of observed longitudinal variation of the N_{IC}/N_{CG} ratio over the US (NLDN/LRF CG measurements and OTD CG+IC measurements) [*Allen and Pickering*, 2002]. For the case of flight 10, balloon-sounding data at Darwin show that an atmospheric temperature of 0°C appeared at an altitude around 5.4 km at 11:00 UT on December 8, although the temperature in a cloud can be different from this value. Because the maximum cloud top altitude of the thunderstorm was 17 km, an N_{IC}/N_{CG} ratio was estimated to be 17. This estimate is generally consistent with results obtained during DUNDEE, conducted at Darwin, in which N_{IC}/N_{CG} ratios derived from five storms showed a systematic increase with total flash rate; the N_{IC}/N_{CG} ratio was 2 to 5 for storms with a total flash rate of 1–3 min^{-1}, while it was 30–40 for deep convection with a total flash rate of 20–50 min^{-1} [*Rutledge et al.*, 1992]. A range of uncertainty for this N_{IC}/N_{CG} estimate was estimated to be a factor between 0.6 and 1.4, which is derived by examining the variability in cloud top altitude where lightning was detected and by referring to the variance of individual data used by *Price and Rind* [1993].

[46] During the lightning event for flight 10, the total number of lightning flashes detected by GPATS was 3260, which took place over the Gulf of Carpentaria between 10:00–14:00 on December 8. When an N_{IC}/N_{CG} ratio of 17 is used, a total flash number ($N_{IC} + N_{CG}$) of 57,400 is obtained. This value is a factor of 10 and 5 times greater than that for the STERAO-A July 10 event [*Defer et al.*, 2001] and the CRYSTAL-FACE July 29 event [*Ridley et al.*, 2004], respectively (Table 1). When a total flash number ($N_{IC} + N_{CG}$) of 57,400 is used for equation (3), the NO production rate P is estimated to be 0.57×10^{25} and 1.9×10^{25} NO molecules per flash for the 11.5–14 km and 0–16 km ranges, respectively (Tables 1 and 2, see discussion in section 4.6 to derive the estimate for the 0–16 km range). Furthermore, when a global lightning flash frequency of 44 flashes s^{-1} [*Christian et al.*, 2003] is used for equation (1), we obtain a global lightning NO production rate of 0.62 Tg(N) yr^{-1} for the 0–16 km range. This value is a factor of 8 smaller than the *IPCC* [2001] recommendation of 5 Tg(N) yr^{-1}.

[47] When the uncertainty in the GPATS flash estimation is considered, this estimate can be used as the lower-limit estimate. To evaluate the range of uncertainties in the NO production rate estimate, we made another estimate. If 60% of the positive CG flashes detected by GPATS were in fact IC flashes, as was the case during the EULINOX experiment [*Thery*, 2001], the NO production rates P given above should be increased by a factor of 2.3. Although a fraction

of positive CG flashes within the total CG flashes of 87% is still much greater than the usual case (about 10%, see description in section 2.2), this represents the upper-limit estimate for this study. When this value is used for flight 10 data, the global lightning NO production rate of 1.4 Tg(N) yr^{-1} for the 0–16 km range is estimated.

[48] The same estimation procedure was also applied to flight 13 data. First we assume that all of the GPATS-detected lightning flashes are CG flashes, then the number of total flashes was estimated using equation (4). The altitudes of most of the clouds for the flight 13 event were 14 km, although clouds as high as 16.5 km were also seen in limited areas (Figure 16). Using equation (4), an N_{IC}/N_{CG} ratio of 6 was obtained and the total lightning flash $N_{IC} + N_{CG}$ becomes 2750. The NO production rate P is then estimated using equation (3) to be 6.5×10^{25} and 21×10^{25} NO molecules per flash for the 11.5–14 km and 0–16 km ranges, respectively. When a global lightning flash frequency of 44 flashes s^{-1} is used for equation (1), a global lightning NO production rate of 6.9 Tg(N) yr^{-1} was obtained for the 0–16 km range. Because of the relatively low flash number (402 GPATS-detected flashes for two-hour storm activity), it is unlikely that many IC flashes are included in this number. However, if we simply adopt the assumption used for the flight 10 analysis, in which 60% of positive CG flashes detected by GPATS were IC flashes, an estimation of the production rate increased by a factor of 2.3. Using those assumptions, the global NO production rate becomes 16 Tg(N) yr^{-1}.

[49] Finally a difference in the NO production rates between the two thunderstorms is discussed. In general, a higher NO production rate per single lightning flash was reported for more intense thunderstorms [e.g., *Ridley et al.*, 2004]; however, a lower production rate was obtained for more intense thunderstorm (flight 10) in this study (0.62–1.4 Tg(N) yr^{-1} and 6.9–16 Tg(N) yr^{-1} for flights 10 and 13, respectively, Tables 1 and 2). Uncertainties in lightning flash number are relatively large in this study, as described in section 2.2 and in Appendix. In fact, although the total amount of NO_x produced from these two thunderstorms differs by a factor of 1.8 (greater for flight 10, Tables 1 and 2), the total lightning flash counts ($N_{IC} + N_{CG}$) differs by a factor of 21, resulting in NO production rates which are different by a factor of 11. However, the comparison of satellite-derived cloud images and radar echo images between the thunderstorms for flights 10 and 13 (Figures 10, 12, 16, and 17) show that there was an apparent difference in intensities of these two thunderstorms. The lightning flash counts for flight 10 thunderstorm can be greater by a factor of more than 2, although the total amount of NO_x produced was greater for flight 10 event only by a factor of 1.8, and therefore, the higher production rate for flight 13 was not simply due to an error in GPATS detection. Consequently, the range in the estimates given in Tables 1 and 2 is considered to be the range of uncertainty in our estimates. Because of the factor of 11 difference in the NO production rate estimates for the two thunderstorm events, it is hard to generalize these values for lightning events over the globe. Although we attempted to provide the global estimates of lightning NO production, one should carefully use these values.

4.8. Uncertainties due to Difference in Production Rates of CG and IC Flashes

[50] In this section, we discuss the uncertainty from the possible difference between the production rates of IC and CG flashes, namely P_{IC} and P_{CG}. As described in section 1, when a difference is considered, one uses equation (2) to estimate the global NO production rate, rather than using equation (1). However, in this case we need to provide both P_{IC} and P_{CG} values, but this is impossible in this study. Thus we examined the range of P_{IC}/P_{CG} values reported in literature to determine a possible error in the estimate of the global production rate. *Price et al.* [1997] proposed P_{IC}/P_{CG} to be 0.1 from theoretical calculations, and this value has been widely used in global CTM calculations. Recent observations, on the other hand, suggest that P_{IC}/P_{CG} is likely greater, possibly as large as unity [*DeCaria et al.*, 2000; *Fehr et al.*, 2004], although this value can depend on the method used to detect IC flashes. We therefore adopted a range for P_{IC}/P_{CG} to be between 0.1 and 1. Note that when $P_{IC}/P_{CG} = 1$, equation (2) becomes identical to equation (1), because the NO production rate is common ($P = P_{CG} = P_{IC}$), and a total flash rate is the sum of IC and CG flash rates ($f = f_{CG} + f_{IC}$). Consequently, the estimates given in the previous section using a global lightning flash frequency of 44 flashes s^{-1} [*Christian et al.*, 2003] do not have to be changed. Therefore we should consider only the effect of using $P_{IC}/P_{CG} = 0.1$ on the estimation of the global NO production rate G.

[51] From our observations (e.g., flight 10), the total mass of atomic nitrogen (N), g_1 produced in the form of NO molecules by lightning is expressed as follows:

$$g_1 = N_1 P\{\beta_1 + (1 - \beta_1)\alpha\} \tag{5}$$

where $N_1 = N_{CG} + N_{IC}$, $\beta_1 = N_{CG}/N_1$, $P = P_{CG}$, and $\alpha = P_{IC}/P_{CG}$. On the other hand, the global NO production rate G given in equation (2) can be written as follows.

$$G = fP\{\beta + (1 - \beta)\alpha\} \tag{6}$$

where $f = f_{CG} + f_{IC}$ (global total flash rate) and $\beta = f_{CG}/f$. P and α are common between equations (5) and (6). From these two equations, (5) and (6), one can easily derive the following equations.

$$G = f \cdot \frac{g_1}{N_1} \cdot \gamma$$
$$\gamma \equiv \frac{\beta + (1 - \beta) \cdot \alpha}{\beta_1 + (1 - \beta_1) \cdot \alpha} \tag{7}$$

[52] The parameter γ in equation (7) can be considered as a correction factor for the NO production rate, which is necessary when the P_{IC}/P_{CG} ratio (α) deviates from unity. When $\alpha = P_{IC}/P_{CG} = 1$, γ becomes unity and g_1/N_1 becomes equal to $P = P_{CG} = P_{IC}$.

[53] Now one can consider the case for $\alpha = P_{IC}/P_{CG} = 0.1$. In this case, we need to estimate $\beta_1 = N_{CG}/N$ and $\beta = f_{CG}/f$ to calculate γ in equation (7). In the case of flight 10,

$\beta_1 = N_{CG}/N = 1/(1 + 17) = 0.056$ was derived (section 4.7). Also, the global average of the f_{IC}/f_{CG} ratio has been reported in the literature. *Nesbitt et al.* [2000] used the total lightning flash frequency ($f_{IC} + f_{CG}$) obtained by OTD and the empirical expression of the f_{IC}/f_{CG} ratio as a function of latitude proposed by *Mackerras et al.* [1998] to derive a global averaged f_{IC}/f_{CG} ratio of 3.5 ($\beta = f_{CG}/f = 0.22$). This result is in agreement with f_{IC}/f_{CG} ratio of 3.3 ($\beta = 0.23$) derived by *Allen and Pickering* [2002]; they examined lightning flash rate parameterizations in a global CTM and their results (Table 4 in *Allen and Pickering* [2002]) suggested that the global average f_{IC}/f_{CG} ratio is 3.3 when their best method (MFLUX method) is used in conjunction with the N_{IC}/N_{CG} parameterization proposed by *Price and Rind* [1993] (equation (4)). When $\beta = 0.23$ is used with $\alpha = P_{IC}/P_{CG} = 0.1$, γ in equation (6) is calculated to be 2.0 for the case of flight 10. This result indicates that even when estimates differing by a factor of 10 are used for P_{IC}/P_{CG} (1 or 0.1), the resulting correction γ is only a factor of 2.0; consequently, the global lightning NO production rate G changes by a factor of 2.0. This is because the estimate of the absolute value of P_{CG} and the P_{IC}/P_{CG} ratio are coupled. In summary, when results from recent studies of $P_{IC}/P_{CG} = 1$ [*DeCaria et al.*, 2000] are considered, our estimate provided in the previous section (Tables 1 and 2) is likely to be reasonable. Our estimate should be increased by a factor of 2.0 when the conventionally used P_{IC}/P_{CG} ratio of 0.1 is adopted for flight 10. We should increase the global production rate because the number fraction of CG flashes ($\beta = f_{CG}/f$) is greater in the global average than that for the case of flight 10.

[54] Note that because the N_{IC}/N_{CG} ratio for the flight 10 thunderstorm is 17, which is much greater than the global average f_{IC}/f_{CG} ratio of 3.3, γ becomes as large as 2.0. When the N_{IC}/N_{CG} ratio is closer to the global average f_{IC}/f_{CG} ratio of 3.3, γ becomes closer to unity and the error in the estimate of G due to the uncertainty in $\alpha = P_{IC}/P_{CG}$ value becomes smaller. In fact, in the case of flight 13, the N_{IC}/N_{CG} ratio is 6 and γ is 1.3. Furthermore, when the N_{IC}/N_{CG} ratio estimate is equal to the global flash ratio f_{IC}/f_{CG} ($\beta_1 = \beta$), γ becomes unity and the choice of $\alpha = P_{IC}/P_{CG}$ does not introduce any error into the estimate of G.

4.9. Note for NO Production Rate Estimation

[55] It is noted that differences in the method to estimate IC flash counts in various studies can result in systematic differences in estimates of the NO production rates, and therefore, comparison of the estimates shown in Table 1 should be carefully made. Furthermore, when the satellite-derived lightning flash frequency (f in equation (1) or f_{IC} in equation (2)) is utilized in the global lightning NO production estimate (G in equation (1) or (2)), one should use IC flash counts in a way comparable to that of satellite observations for the NO production rate estimates (P in equation (1) or P_{IC} in equation (2)). For example, *Ridley et al.* [2004] used a climatological IC/CG flash count ratio (N_{IC}/N_{CG} ratio = 2.25) to derive the IC flash count from the US NLDN-derived CG flash count, where the climatological ratio had been derived by comparing US NLDN-derived CG flash counts and satellite-borne OTD derived CG + IC flash counts [*Boccippio et al.*, 2001]. Because the total lightning flash count ($N_{CG} + N_{IC}$) over the globe was derived from the OTD satellite measurement (44 ± 5 flashes s^{-1}, [*Christian et al.*, 2003]), the NO production rate P estimated by *Ridley et al.* [2004] can be used directly to estimate the global NO production rate from satellite-derived flash counts using equation (1), although spatial and temporal changes in the N_{IC}/N_{CG} ratio can introduce some errors when P_{IC}/P_{CG} deviates from unity (see discussion in section 4.8).

[56] On the other hand, IC flash counts detected by the VHF interferometer operated by the French Office Nationale d'Etudes et de Recherches Aerospatiales (ONERA) were used by *DeCaria et al.* [2000] and *Skamarock et al.* [2003]. Because the interferometer likely detects many more flashes owing to its higher sensitivity than the satellite-borne OTD (N_{IC}/N_{CG} ratio = 7–500) [*Dye et al.*, 2000], the estimated NO production rate per flash tends to be smaller and it cannot be used to accurately estimate the global production rate using the OTD-derived global flash rate without knowing the relationship between flash counts from ONERA and OTD.

[57] In this study, we use the empirical expression for the N_{IC}/N_{CG} ratio proposed by *Price and Rind* [1993] (equation (4)) to estimate IC flash counts from observed CG flash counts, as described in section 4.7. As also described in section 4.7, this expression has been tested to some extent by *Allen and Pickering* [2002] over the US by comparing satellite-borne OTD IC+CG measurements and NLDN/LRF CG measurements. Although the expression has never been tested in the tropics, the IC flash counts estimated in this study are considered to be comparable to the satellite measurements.

4.10. Impact on Ozone

[58] The average NO_x mixing ratio at altitudes between 11.5 and 14 km was 291 ± 215 pptv and 209 ± 225 pptv for flights 10 and 13, respectively (Tables 2 and 3). On the other hand, the average NO_x mixing ratio in the study (Figure 1) in the same altitude range was 41.0 ± 41.9 pptv when data from flights 10 and 13 were excluded (Table 3). This value is slightly higher than the average of 15 ± 6 pptv in air outside of the high-NO_x air observed during flight 10 (section 4.2.2), suggesting the presence of regional influences of lightning NO production. Using these values, the diurnal average O_3 production/loss rate was calculated using the box model described in section 2.1. As a result, the net production rate of 1.95 and 1.52 ppbv day^{-1} was obtained for flights 10 and 13, respectively, while it was 0.53 ppbv day^{-1} for the study area (Table 3). Considering the area of the high-NO_x air regions for the two events (140 × 620 km^2 and 170 × 400 km^2) and the relatively long NO_x lifetime of about a week, NO production by thunderstorms is considered to increase the regional NO_x level and have a significant impact on O_3 chemistry in the tropics.

[59] It is noted that although the NO_x concentration is greater for flight 10 as compared to that in the study area by a factor of 7.1, the diurnal average O_3 production rate is greater only by a factor of 3.3. This is because the O_3 production rate depends not only on the NO concentration but also peroxy radical concentrations. In general, precursors of the hydroperoxy radical (HO_2), such as H_2O, are transported from the lower troposphere to the middle and upper troposphere within a convective system, and this mechanism can enhance

Table 3. Diurnal Average Ozone Production ($P(O_3)$) and Loss ($L(O_3)$) Rates at Altitudes Between 11.5 and 14 km

	Flight 10	Flight 13	Others (Study Area)
NO_x (pptv)	291 ± 224	209 ± 225	41.0 ± 41.9
$P(O_3)$ (ppbv day^{-1})	2.07 ± 0.90	1.65 ± 0.81	0.62 ± 0.32
$L(O_3)$ (ppbv day^{-1})	0.13 ± 0.04	0.13 ± 0.03	0.09 ± 0.05
$P(O_3)$-$L(O_3)$ (ppbv day^{-1})	1.95 ± 0.88	1.52 ± 0.80	0.53 ± 0.31

the O_3 production rate in the presence of elevated levels of NO produced by lightning [e.g., *Jaeglé et al.*, 1999]. However, during the BIBLE-C experiment, H_2O is transported into middle and upper troposphere quite efficiently within the study area (section 3). As a result, H_2O and HO_x concentrations were not necessarily higher for the flight 10 and 13 cases as compared to those of the rest of the flights, and HO_2 concentrations were even lower due to higher NO concentrations during these two flights, resulting in reduction in the O_3 production rate. This result suggests that when O_3 production rates calculated for flight 10 and 13 are compared with those obtained within dry tropical air that is not influenced by recent convection, the enhancement should be even greater.

5. Summary

[60] To study the influences of lightning NO production in the tropical Western Pacific, the BIBLE-C aircraft campaign was conducted in December 2000 using the G-II research aircraft, and in total, eight intensive flights were made from Darwin, Australia (12°S, 131°E). Because of the earlier-than-average onset of the summer monsoon season, the experiments were carried out in the monsoonal regime. Measurements of NO and NO_y were made together with O_3, CO, H_2O, CH_4, NMHCs, and some other parameters on board the aircraft. Photostationary-state NO_2 mixing ratios were calculated using a box model, from which it was found that 95% of NO_x was in the form of NO at an altitude of 12.5 km during our measurements.

[61] During two flights (flights 10 and 13 made on December 9 and 11–12, respectively), enhancements of NO_x (NO + NO_2) up to 1000 or 1600 pptv (10-s data) were observed at altitudes between 11.5 and 14 km. In these cases, NO_y mixing ratios reached 1500 and 2000 pptv, respectively, and NO_x/NO_y ratios of 0.7–0.8 were observed. Air in which NO_x exceeded 100 pptv extended over 620 × 140 km^2 and 400 × 170 km^2 (wind direction × perpendicular direction). To our knowledge, it has never before been reported that high-NO_x air produced by a single thunderstorm system extended over such a wide area, at least in the tropics. This suggests a significant impact of lightning NO production on NO_x levels in the tropics. The average NO_x mixing ratios in these areas were 291 and 209 pptv at 11.5–14 km. The CO mixing ratios were generally higher in air influenced by convection (flight 10 and 13 data) than those in pristine air originating from the Central Pacific (other flight data in the study area). However, influences of the vertical transport of lower-tropospheric air on NO_x levels was estimated to be as low as 28 pptv when the relationship between NO_x and CO data obtained at altitudes lower than 4 km was examined. From these NO_x values and the estimated area of lightning influence, the total NO amount produced by individual lightning events was estimated to be 3.3 and 1.8 × 10^{29} NO molecules for flights 10 and 13, respectively, in the 11.5–14 km altitude range. Because of wind shear at altitudes between 8 and 9 km and the limit of the altitude range of our measurements, lightning influences at altitudes below 11.5 and above 14 km cannot be estimated in this study. When we use the vertical profile of lightning NO_x mass distribution developed by *Pickering et al.* [1998], the total number of NO molecules within the entire tropospheric column (0–16 km) is a factor of 3.2 greater than that within 11.5 and 14 km. The uncertainties for the NO_x production estimates for 11.5–14 km and for the total column amounts were estimated to be as large as a factor of 2 and 3, respectively.

[62] GMS cloud (brightness temperature) data and ground-based lightning measurements by GPATS indicate that in the cases of both flights 10 and 13, there were intense lightning events over the coast of the Gulf of Carpentaria, which took place upstream from our measurement area 10 to 14 h prior to the measurements. In the case of flight 10, the cloud top likely reached the tropopause at 17 km, and the region of the near-tropopause cloud extended to 190 × 120 km^2 during the mature phase. The thunderstorm lasted for 3 h. In the case of flight 13, convection activity was less intense and most of cloud tops were around 14 km.

[63] For the flight 10 and 13 thunderstorms, GPATS-detected 3260 and 402 lightning flashes, respectively. In this study we made two estimates for the NO production rate per single lightning flash. In the first estimate we used GPATS-detected flashes as CG flashes, and in the second estimate we assumed 60% of the positive flashes were in fact IC flashes based on the report by *Thery* [2001]. This is because although GPAST (LPATS) is supposed to detect only CG flashes, the fact that 95% of the GPATS-detected flashes had positive polarity is contrary to general CG flash features in which only 10% of CG flashes have positive polarity. We estimated the total lightning flash counts (N_{IC} + N_{CG}) from CG flash count (N_{CG}) using an empirical parameterization of the N_{IC}/N_{CG} ratio developed by *Price and Rind* [1993] to obtain the N_{IC}/N_{CG} value of 17 and 6 for the flight 10 and 13 cases, respectively. As a result, the column NO production rate (0–16 km) per single lightning flash was estimated to be 1.9–4.4 and 21–49 × 10^{25} NO molecules per single flash for these two flight data sets. Using a global flash rate of 44 flashes s^{-1} [*Christian et al.*, 2003], the global NO production rate was estimated to be 0.62–1.4 and 6.9–16 Tg(N) yr^{-1}. A large range in the estimates is due to large uncertainties in the GPATS lightning data. Consequently, care must be made when these estimates on NO production rate are referred, although they are the best estimates from our study. A range of the additional uncertainty is considered to be as large as a factor of 0.2–10 when the uncertainties in the amount of column-produced NO in this study (a factor of 0.3–3 in the global production rate), the N_{IC}/N_{CG} ratio (a factor of 0.8–1.7), and the P_{IC}/P_{CG} ratio (a factor of 1–2) are considered.

[64] The diurnally averaged net O_3 production rate at 12.5 km was calculated to be 1.95 and 1.52 ppbv day^{-1} for flights 10 and 13, respectively. These values are systemat-

ically greater than the average in the study area of 0.53 ppbv day^{-1}, suggesting a significant impact on the O_3 production rate over the tropical Western Pacific.

Appendix A

[65] Statistical analyses on the fraction of negative/positive flashes are made for the Australian GPATS data using one-month data obtained in December 2000, when the BIBLE-C experiment was conducted (Table A1). As described in section 3, northern Australia was under monsoonal meteorological conditions and the lightning activity was generally similar throughout this month (Figure 3). The first statistics is made for data obtained within an area in which lightning events for flight 10 and 13 took place, 12–18°S and 132–140°E (denoted as ''near Darwin'' in Table A1). Of 82401 lightning flashes, only 20% of GPATS-detected flashes were negative. This is higher than that for the flight 10 and 13 thunderstorms (5.7 and 4.3%, respectively), however, it is still much lower than the typically observed value of 90% [*Petersen and Rutledge*, 1992; *Zajac and Rutledge*, 2001]. Lightning flashes in this area were detected by three GPATS receivers located in northern Australia (shown by open circles in Figure 1). When the second statistics is made for data obtained within a triangular area surrounded by these three receivers, a similar result (negative flashes are 28%, Table A1) is obtained. This result suggests that the very low fraction of negative flashes near Darwin was not simply due to the long distance from the three receivers (about 400–600 km), but due to the peculiar characteristics of the three receivers. When the third statistics is made for data obtained within an area ''near Sydney'' (27–38°S and 146–153°E), a fraction of negative flashes of 55% is obtained (Table A1). Although this is higher than the result near Darwin, it is still lower than the typical value of 90%. Considering these results, there is a possibility that some negative CG flashes detected near Darwin during BIBLE-C were mislabeled as positive CG flashes and/or a portion of the IC flashes were mislabeled as positive CG flashes.

[66] We also compared simultaneous measurements made by GPATS and Lightning Imaging Sensor (LIS) onboard the Tropical Rainfall Measuring Mission (TRMM) satellite [*Christian et al.*, 1999] using one-month data obtained in December 2000. The LIS is considered to measure both CG and IC flashes, while GPATS is considered to measure only CG flashes. Consequently, the ratio of lightning flash counts between the two measurements can provide some insights into a possible mislabeling of IC flash as CG flash by GPATS measurements. The LIS made measurements once or twice a day (ascending and descending passes) within a part of the ''near Darwin'' area (12–18°S and 132–140°E) and it looked individual 0.5° × 0.5° grid box for a time period of about 80 seconds. Within the December 2000 data obtained in the ''near Darwin'' area, there were only 2 cases in which GPATS detected more than 3 lightning flashes within the LIS viewing area and time period, namely, December 8 and 21. The December 8 case is the exact thunderstorm, which is responsible for the flight 10 event described in section 4.2 (Figure A1). In this case, locations where lightning flashes were detected agree well between the two measurements. GPATS detected 8 flashes within the time period in which LIS detected 30 flashes, resulting in a LIS/GPATS ratio of 3.8. In the other case (December 21), a LIS/GPATS ratio of 18 was obtained. Unfortunately the number of the thunderstorms examined here is too small to derive any conclusion in evaluating GPATS data when and where the BIBLE-C experiment was conducted.

[67] We made further analyses by comparing GPATS measurements with the OTD [*Christian et al.*, 2003] and LIS climatological lightning flash density data (CG + IC flashes km^{-2} day^{-1}), which have been compiled for each month from multi-year data (OTD:1995–1999 and LIS:1998–2005). In Table A2, OTD- and LIS-derived climatology for December is compared with the GPATS-detected lightning flash density obtained in December 2000. Ratios of flash densities ((OTD & LIS)/GPATS) are calculated to be 11 and 9.0 for the ''near Darwin'' area (12–18°S and 132–140°E) and ''near Sydney'' area (27–38°S and 146–153°E), respectively. These values are within a range of the $(N_{IC} + N_{CG})/N_{CG}$ ratios of 18 and 7 estimated for flights 10 (cloud top altitude of 17 km) and 13 (cloud top altitude of 14 km), respectively, using equation (4) proposed by *Price and Rind* [1993]. Because of the earlier-than-average onset of monsoonal meteorological conditions in December 2000 (section 3), the lightning activity in year 2000 could be lower than other years and therefore, (OTD & LIS)/GPATS ratios could be lower if we compare year 2000 data for OTD & LIS and GPATS, although this comparison is not possible due to a sparseness of OTD & LIS data. If we simply assume that all negative GPATS flash

Table A1. Statistics of GPATS-detected Lightning Flashes for December 2000

	Total Flash Counts	Positive Flash Fraction, %	Negative Flash Fraction, %
Near Darwin [a]	82,401	80	20
Within 3 receivers [b]	31,717	72	28
Near Sydney[c]	128,817	45	55
Flight 10 [d]	3260	94	6
Flight 13[d]	402	96	4

[a]12–18°S and 132–140°E.
[b]Triangular area surrounded by the following 3 receivers: Cairns (16.9°S, 145.7°E), Tennant Creek (19.6°S, 134.2°E), and Mt. Isa (20.7°S, 139.5°E), which are shown with open circles in Figure 1.
[c]27–38°S and 146–153°E.
[d]Results for the thunderstorms responsible for flight 10 and 13 data are shown here for comparison. These two thunderstorms took place within the ''near Darwin'' area shown in this table.

Table A2. Statistics of GPATS-detected and LIS Lightning Flash Densities for December

	GPATS, flashes km^{-2} day^{-1} [a]	OTD & LIS, flashes km^{-2} day^{-1}[b]	(OTD & LIS)/GPATS Ratio
Near Darwin [c]	0.0057	0.065	11
Near Sydney [d]	0.0064	0.058	9.0

[a]Statistics of GPATS-detected Lightning Flashes for December 2000.
[b]Climatological data for December obtained by the satellite borne sensors OTD (1995–1999) and LIS (1998–2005). The data was provided with a 2.5° × 2.5° resolution after 110- or 98-day temporal smoothing (OTD and LIS). Data are available from http://thunder.msfc.nasa.gov/data/.
[c]12–18°S and 132–140°E.
[d]27–38°S and 146–153°E.

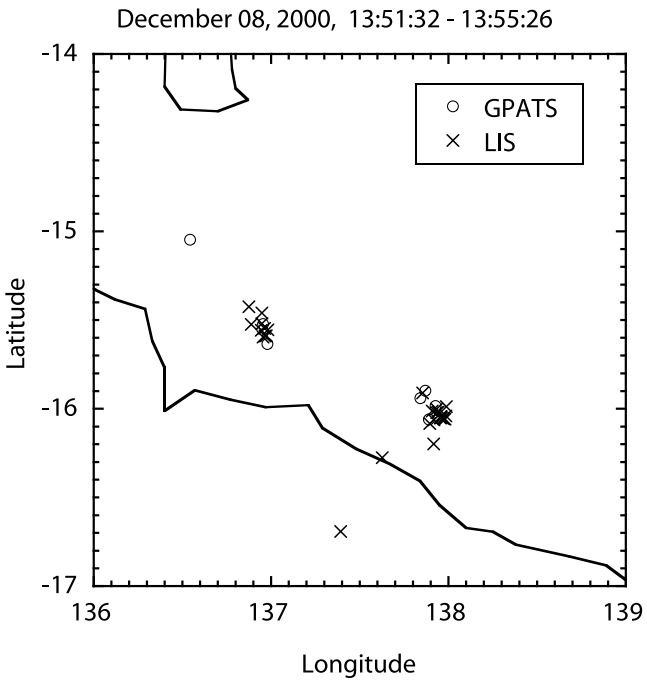

Figure A1. Locations of lightning flashes detected by GPATS system (circles) and the satellite-born sensor LIS (crosses) within a time period between 13:51:32 and 13:55:26 on December 8, 2000. These flashes are part of the thunderstorm activity which is responsible for flight 10 high-NO_x air (Figure 10).

and 40% of positive GPATS flashes are CG flashes (N_{CG}), as assumed in this study in section 4.7, and use OTD & LIS measurements for $N_{IC} + N_{CG}$, a $(N_{IC} + N_{CG})/N_{CG}$ ratio of 22 is obtained for the "near Darwin" area. This is close to an upper limit when we use equation (4) for $(N_{IC} + N_{CG})/N_{CG}$ estimate, because only clouds which reach the tropopause (around 17–18 km) will result in this high ratio. Considering these results and uncertainties in $(N_{IC} + N_{CG})/N_{CG}$ estimates using equation (4), the total lightning flash estimates from GPATS-detected flash counts in this study (section 4.7) are reasonable: in the first estimate we use GPATS-detected lightning flashes as CG flashes and in the second estimate we assume all negative GPATS flashes and 40% of positive GPATS flashes are CG flashes.

[68] **Acknowledgments.** We are indebted to all of the BIBLE participants for their cooperation and support. Special thanks are due to the flight and ground crews of the DAS GII aircraft for helping make this effort a success. We thank Mr. N. Toriyama, M. Kanada, and H. Jindo for their technical assistance with the measurements of NO and NO_y. We also thank Dr. P. May at the Bureau of Meteorology Research Centre in Australia for providing radar echo data and useful comments on them. Lightning data were provided by Global Position and Tracking Systems Pty. Ltd. (GPATS) in Australia. NASA Optical Transient Detector (OTD) and Lightning Imaging Sensor (LIS) data were provided by the Global Hydrology Resource Center (GHRC) at the Global Hydrology and Climate Center, Huntsville, Alabama, USA. Meteorological data were provided by the European Center for Medium-Range Weather Forecasts (ECMWF). Interpolated OLR data were provided by the NOAA/OAR/ESRL PSD, Boulder, Colorado, USA, from their Web site at http://www.cdc.noaa.gov/. This work was supported in part by the Ministry of Education, Culture, Sports, Science, and Technology (MEXT) and Japan Aerospace Exploration Agency (JAXA)/Earth Observation Research Center (EORC). The BIBLE campaigns were conducted under the framework of the International Global Atmospheric Chemistry (IGAC) project (http://www.igac.noaa.gov/).

References

Allen, D. J., and K. E. Pickering (2002), Evaluation of lightning flash rate parameterization for use in a global chemical transport model, *J. Geophys. Res.*, *107*(D23), 4711, doi:10.1029/2002JD002066.

Allen, D., K. Pickering, G. Stenchikov, A. Thompson, and Y. Kondo (2000), A three-dimensional total odd nitrogen (NO_y) simulation during SONEX using a stretched-grid chemical transport model, *J. Geophys. Res.*, *105*, 3815–3876.

Boccippio, D. J., K. L. Cummins, H. J. Christian, and S. J. Goodman (2001), Combined satellite- and surface-based estimation of the intracloud-cloud-to-ground lightning ratio over the continental United States, *Mon. Wea. Rev.*, *129*, 108–122.

Boersma, K. F., H. J. Eskes, E. W. Meijer, and H. M. Kelder (2005), Estimates of lightning NO_x production from GOME satellite observations, *Atmos. Chem. Phys.*, *5*, 2311–2331.

Bond, D. W., S. Steiger, R. Zhang, X. Tie, and R. E. Orville (2002), The importance of NO_x production by lightning in the tropics, *Atmos. Environ.*, *36*, 1509–1519.

Christian, et al. (1999), The Lighting Imaging Sensor, *Proc. 11th Int. Conf. Atmos. Elect.*, Guntersville, AL, International Commission on Atmospheric Electricity, 746–749.

Christian, et al. (2003), Global frequency and distribution of lightning as observed from space by the Optical Transient Detector, *J. Geophys. Res.*, *108*(D1), 4005, doi:10.1029/2002JD002347.

Cummins, K. L., M. J. Murphy, E. A. Bardo, W. L. Hiscox, R. B. Pyle, and A. E. Pifer (1998), A combined TOA/MDF technology upgrade of the U.S. National Lightning Detection Network, *J. Geophys. Res.*, *103*, 9035–9044.

DeCaria, A. J., K. E. Pickering, G. L. Stenchikov, J. R. Scala, J. L. Stith, J. E. Dye, B. A. Ridley, and P. Laroche (2000), A cloud-scale model study of lightning-generated NO_x in an individual thunderstorm during STERAO-A, *J. Geophys. Res.*, *105*, 11,601–11,616.

Defer, E., P. Blanchet, C. Thery, P. Laroche, J. E. Dye, M. Venticinque, and K. L. Cummins (2001), Lightning activity for the July 10, 1996, storm during the Stratosphere-Troposphere Experiment, Radiation, Aerosol, and Ozone-A (STRAO-A) experiment, *J. Geophys. Res.*, *106*, 10,151–10,172.

Dye, J. E., et al. (2000), An overview of the Stratospheric-Tropospheric Experiment: Radiation, Aerosols, and Ozone (STERAO)-Deep Convection experiment with results for the July 10, 1996 storm, *J. Geophys. Res.*, *105*, 10,023–10,045.

Fehr, T., H. Höller, and H. Huntrieser (2004), Model study on production and transport of lightning-produced NO_x in a EULINOX supercell storm, *J. Geophys. Res.*, *109*, D09102, doi:10.1029/2003JD003935.

Grewe, V., D. Brunner, M. Dameris, J. L. Grenfell, R. Hein, D. Shindell, and J. Staehelin (2001), Origin and variability of upper tropospheric nitrogen oxides and ozone at northern mid-latitudes, *Atmos. Environ.*, *35*, 3421–3433.

Höller, H., U. Finke, H. Huntrieser, M. Hagen, and C. Feigl (1999), Lightning-produced NO_x (LINOX): Experimental design and case study results, *J. Geophys. Res.*, *104*, 13,911–13,922.

Huntrieser, H., H. Schlager, C. Feigl, and H. Holler (1998), Transport and production of NO_x in electrified thunderstorms: Survey of previous studies and new observations at midlatitudes, *J. Geophys. Res.*, *103*, 28,247–28,264.

Huntrieser, H., et al. (2002), Airborne measurements of NO_x, tracer species, and small particles during the European Lightning Nitrogen Oxides Experiment, *J. Geophys. Res.*, *107*(D11), 4113, doi:10.1029/2000JD000209.

Intergovernmental Panel on Climate Change (IPCC) (2001), Climate change 2001: The scientific basis, Geneva.

Jaeglé, L., et al. (1999), Ozone production in the upper troposphere and the influence of aircraft during SONEX: Approach of NO_x-saturated condition, *Geophys. Res. Lett.*, *26*, 3081–3084.

Jeker, D. P., L. Pfister, A. M. Thompson, D. Brunner, D. J. Boccippio, K. E. Pickering, H. Wernli, Y. Kondo, and J. Staehelin (2000), Measurements of nitrogen oxides at the tropopause: Attribution to convection and correlation with lightning, *J. Geophys. Res.*, *105*, 3679–3700.

Kawakami, S., et al. (1997), Impact of lightning and convection on reactive nitrogen in the tropical free troposphere, *J. Geophys. Res.*, *102*, 28,367–28,384.

Kita, K., et al. (2002), Photochemical production of ozone in the upper troposphere in association with cumulus convection over Indonesia, *J. Geophys. Res.*, *107*(D3), 8400, doi:10.1029/2001JD000844.

Ko, M., W. Hu, J. Rodriguez, Y. Kondo, M. Koike, K. Kita, S. Kawakami, D. Blake, S. Liu, and T. Ogawa (2002), Photochemical ozone budget during the BIBLE-A and B campaign, *J. Geophys. Res.*, *107*(D23), 8404, doi:10.1029/2001JD000800.

Koike, M., et al. (2000), Impact of aircraft emissions on reactive nitrogen over the North Atlantic Flight Corridor region, *J. Geophys. Res.*, *105*, 3665–3677.

Koike, M., et al. (2002a), Reactive nitrogen over the tropical Western Pacific: Influence from lightning and biomass burning, *J. Geophys. Res.*, *107*(23), 8403, doi:10.1029/2001JD000823.

Koike, M., et al. (2002b), Redistribution of reactive nitrogen in the Arctic lower stratosphere in the 1999–2000 winter, *J. Geophys. Res.*, *107*(D20), 8275, doi:10.1029/2001JD001089.

Koike, M., et al. (2003), Export of anthropogenic reactive nitrogen and sulfur compounds from the East Asia region in spring, *J. Geophys. Res.*, *108*(D20), 8789, doi:10.1029/2002JD003284.

Kondo, Y., S. Kawakami, M. Koike, D. W. Fahey, H. Nakajima, N. Toriyama, M. Kanada, Y. Zhao, G. W. Sachse, and G. L. Gregory (1997), The performance of an aircraft instrument for the measurement of NO_y, *J. Geophys. Res.*, *102*, 28,663–28,671.

Kondo, Y., M. Ko, M. Koike, S. Kawakami, and T. Ogawa (2002), Preface to special section on Biomass Burning and Lightning Experiment (BIBLE), *J. Geophys. Res.*, *107*(D23), 8397, doi:10.1029/2002JD002401.

Labrador, L. J., R. von Kuhlmann, and M. G. Lawrence (2005), The effects of lightning-produced NO_x and its vertical distribution on atmospheric chemistry: Sensitivity simulations with MATCH-MPIC, *Atmos. Chem. Phys.*, *5*, 1815–1834.

Lamarque, et al. (1996), Three-dimensional study of the relative contributions of the different nitrogen sources in the troposphere, *J. Geophys. Res.*, *101*, 22,955–22,968.

Lange, et al. (2001), Detection of lightning-produced NO in the midlatitude upper troposphere during STREAM 1998, *J. Geophys. Res.*, *106*, 27,777–27,785.

Levy, H., II, W. J. Moxim, K. A. Klonecki, and P. S. Kashibhatla (1999), Simulated tropospheric NO_x: Its evaluation, global distribution and individual source contributions, *J. Geophys. Res.*, *104*, 26,279–26,306.

MacGorman, D. R., and W. D. Rust (1998), The Electrical Nature of Storms, Oxford Univ. Press.

Mackerras, D., M. Darveniza, R. E. Orville, E. R. Williams, and S. J. Goodman (1998), Global lightning: Total, cloud and ground flash estimates, *J. Geophys. Res.*, *103*, 19,791–19,809.

Marshall, J. S., and W. M. Palmer (1948), *J. Meteorol.*, *5*, 165–166.

Miyazaki, Y., et al. (2005), Contribution of particulate nitrate to airborne measurements of total reactive nitrogen, *J. Geophys. Res.*, *110*, D15304, doi:10.1029/2004JD005502.

Nesbitt, S. W., R. Zhang, and R. E. Orville (2000), Seasonal and global NO_x production by lightning estimated from the optical transient detector (OTD), *Tellus*, *52B*, 1206–1215.

Oshima, N., et al. (2004), Asian chemical outflow to the Pacific in late spring observed during the PEACE-B aircraft mission, *J. Geophys. Res.*, *109*(D23), D23S05, doi:10.1029/2004JD004976.

Petersen, W. A., and S. A. Rutledge (1992), Some characteristics of cloud-to-ground lightning in tropical Northern Australia, *J. Geophys. Res.*, *97*, 11,553–11,560.

Pickering, K. E., Y. Wang, W.-K. Tao, C. Price, and J.-F. Muller (1998), Vertical distributions of lightning NO_x for use in regional and global chemical transport models, *J. Geophys. Res.*, *103*, 31,203–31,216.

Price, C., and D. Rind (1992), A simple lightning parameterization for calculating global lightning distributions, *J. Geophys. Res.*, *97*, 9919–9933.

Price, C., and D. Rind (1993), What determines the cloud-to-ground lightning fraction in thunderstorms?, *Geophys. Res. Lett.*, *20*, 463–466.

Price, C., J. Penner, and M. Prather (1997), NO_x from lightning, 1. Global distribution based on lightning physics, *J. Geophys. Res.*, *102*, 5929–5941.

Ridley, B. A., J. E. Dye, J. G. Walega, J. Zheng, F. E. Grahek, and W. Rison (1996), On the production of active nitrogen by thunderstorms over New Mexico, *J. Geophys. Res.*, *101*, 20,985–21,005.

Ridley, B., et al. (2004), Florida thunderstorms: A faucet of reactive nitrogen to the upper troposphere, *J. Geophys. Res.*, *109*, D17305, doi:10.1029/2004JD004769.

Rutledge, and MacGorman (1988), Cloud-to-ground lightning activity in the 10–11 June 1985 convective system observed during the Oklahoma-Kansas PRE-STORM project, *Mon. Weather Rev.*, *116*, 1393–1408.

Rutledge, S. A., E. R. Williams, and T. D. Keenan (1992), The Down Under Doppler and Electricity Experiment (DUNDEE): Overview and preliminary results, *Bull. Am. Meteorol. Soc.*, *73*, 3–16.

Simpson, I. J., et al. (2000), Nonmethane hydrocarbon measurements in the North Atlantic flight corridor during SONEX, *J. Geophys. Res.*, *105*, 3785–3794.

Skamarock, W. C., J. E. Dye, E. Defer, M. C. Barth, J. L. Stith, B. A. Ridley, and K. Baumann (2003), Observational- and modeling-based budget of lightning-produced NO_x in a continental thunderstorm, *J. Geophys. Res.*, *108*(D10), 4305, doi:10.1029/2002JD002163.

Takegawa, N., et al. (2001), Airborne vacuum ultraviolet resonance fluorescence instrument for in situ measurement of CO, *J. Geophys. Res.*, *106*, 24,237–24,244.

Thery, C. (2001), Evaluation of LPATS data using VHF interferometric observations of lightning flashes during the Eulinox experiment, *Atmos. Res.*, *56*, 397–409.

Tie, X., R. Zhang, G. Brasseur, L. Emmons, and W. Lei (2001), Effects of lightning on reactive nitrogen and nitrogen reservoir species in the troposphere, *J. Geophys. Res.*, *106*, 3167–3178.

Tomikawa, Y., and K. Sato (2005), Design of the NIPR trajectory model, *Polar Metorol. Glaciology*, *19*, 120–137.

Uman, M. A. (1987), The Lightning Discharge, Dover Publication Inc..

Volz-Thomas, A., A. Lerner, H.-W. Pätz, M. Schultz, D. S. McKenna, R. Schmitt, S. Madronich, and E. P. Röth (1996), Airborne measurements of the photolysis frequency of NO2, *J. Geophys. Res.*, *101*, 18,613–18,627.

Wang, Y., D. J. Jacob, and J. A. Logan (1998), Global simulation of tropospheric O_3-NO_x-hydrocarbon chemistry. 2. Model evaluation and global ozone budget, *J. Geophys. Res.*, *103*, 10,727–10,755.

Zajac, B. A., and S. A. Rutledge (2001), Cloud-to-ground lightning activity in the contiguous United States from 1995 to 1999, *Mon. Weather Rev.*, *129*, 999–1019.

Zhang, X., J. H. Helsdon, and R. D. Farley (2003), Numerical modeling of lightning-produced NO_x using an explicit lightning scheme: 1. Two-dimensional simulation as a ''proof of concept'', *J. Geophys. Res.*, *108*(D18), 4579, doi:10.1029/2002JD003224.

D. R. Blake, Department of Chemistry, University of California-Irvine, Irvine, CA 92697-2025, USA. (drblake@uci.edu)

T. Kashihara, M. Koike, and S. Kudoh, Department of Earth and Planetary Science, Graduate School of Science, University of Tokyo, Hongo 7-3-1, Bunkyo-ku, Tokyo 113-0033, Japan. (koike@eps.s.u-tokyo.ac.jp; skudoh@eps.s.u-tokyo.ac.jp)

S. Kawakami and T. Ogawa, Earth Observation Research and Application Center, Japan Aerospace Exploration Agency, 1-8-10 Harumi, Tokyo 104-6023, Japan. (kawakami.shuji@jaxa.jp; ogawa.toshihiro@jaxa.jp)

Z. Kawasaki, Department of Communications Engineering, Graduate School of Engineering, Osaka University, Yamada-Oaka 2-1, Suita, Osaka 565-0871, Japan. (zen@comm.eng.osaka-u.ac.jp)

K. Kita, Department of Environmental Sciences, Faculty of Science, Ibaraki University, 2-1-1 Bunkyo, Mito, Ibaraki 310-8512, Japan. (kita@env.sci.ibaraki.ac.jp)

M. W. Ko, Langley Research Center, Mail Stop 401B, 21 Langley Boulevard, Hampton, VA 23681-2199, USA. (malcolm.k.ko@nasa.gov)

Y. Kondo, Y. Miyazaki, and N. Takegawa, Research Center for Advanced Science and Technology, University of Tokyo, 4-6-1 Komaba, Meguro, Tokyo 153-8904, Japan. (kondo@atmos.rcast.u-tokyo.ac.jp; yuzom@atmos.rcast.u-tokyo.ac.jp; takegawa@atmos.rcast.u-tokyo.ac.jp)

B. Liley, National Institute of Water and Atmospheric Research Ltd, Private Bag 50061, Omakau, Central Otago, Lauder, New Zealand. (b.liley@niwa.co.nz)

N. Nishi, Department of Earth and Planetary Science, Graduate School of Science, Kyoto University, Kitashirakawa-Oiwakecho, Sakyo-ku, Kyoto 606-8502, Japan. (nishi@kugi.kyoto-u.ac.jp)

T. Shirai, National Institute for Environmental Studies, 16-2 Onogawa, Tsukuba, Ibaraki 305-8506, Japan. (tshirai@nies.go.jp)